5-Imino-1,2,4-Thiadiazoles: First Small Molecules As Substrate Competitive Inhibitors of Glycogen Synthase Kinase 3

ARTICLE *in* JOURNAL OF MEDICINAL CHEMISTRY · FEBRUARY 2012

Impact Factor: 5.45 · DOI: 10.1021/jm201463v · Source: PubMed

Journal of Medicinal Chemistry

Article

pubs.acs.org/jmc

5-Imino-1,2,4-Thiadiazoles: First Small Molecules As Substrate Competitive Inhibitors of Glycogen Synthase Kinase 3

Valle Palomo,[†] Daniel I. Perez,[†] Concepcion Perez,[†] Jose A. Morales-Garcia,[‡] Ignacio Soteras,[†] Sandra Alonso-Gil,[‡] Arantxa Encinas,[†] Ana Castro,[†] Nuria E. Campillo,[†] Ana Perez-Castillo,[‡] Carmen Gil,*[,†] and Ana Martinez*[,†]

[†]Instituto de Química Médica-CSIC, Juan de la Cierva 3, 28006 Madrid, Spain

[‡]Instituto de Investigaciones Biomédicas (CSIC-UAM) and Centro de Investigación Biomédica en Red sobre Enfermedades Neurodegenerativas (CIBERNED), Arturo Duperier 4, 28029 Madrid, Spain

Supporting Information

ABSTRACT: Cumulative evidence strongly supports that glycogen synthase kinase-3 (GSK-3) is a pathogenic molecule when it is up-dysregulated, emerging as an important therapeutic target in severe unmet human diseases. GSK-3 specific inhibitors might be promising effective drugs for the treatment of devastating pathologies such as neurodegenerative diseases, stroke, and mood disorders. As GSK-3 has the ability to phosphorylate primed substrates, small molecules able to bind to this site should be perfect drug candidates, able to partially block the activity of the enzyme over some specific substrates. Here, we report substituted 5-imino-1,2,4-thiadiazoles as the first small molecules able to inhibit GSK-3 in a substrate competitive manner. These compounds are cell permeable, able to decrease inflammatory activation and to selectively differentiate neural stem cells. Overall, 5-imino-1,2,4-thiadiazoles are presented here as new molecules able to decrease neuronal cell death and to increase endogenous neurogenesis blocking the GSK-3 substrate site

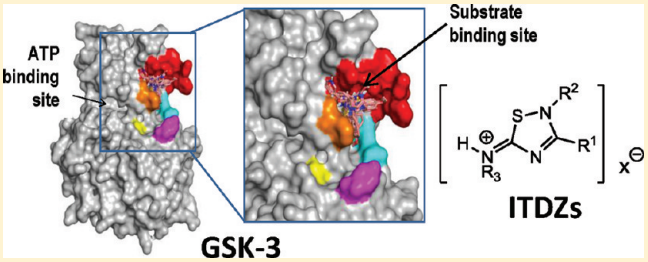

INTRODUCTION

Glycogen synthase kinase 3 (GSK-3) is a protein kinase originally identified and named for its ability to inactivate by phosphorylation the metabolic enzyme, involved in the last step of glycogen synthesis, called glycogen synthase.[1] In the last two decades, much information has been gained about the physiological and pathological role of this ubiquitous serine/threonine kinase and its inhibitors.[2] More recently, GSK-3 has been found to play an important role in the central nervous system (CNS). It modulates many aspects of neuronal function, such as gene expression, neurogenesis, synaptic plasticity, neuronal structure, and neuronal death and survival.[3] Moreover, cumulative evidence strongly supports that GSK-3 is a pathogenic molecule in this tissue when dysregulated. Thus, GSK-3 emerges as an important therapeutic target in different severe human diseases such as neurodegenerative diseases, stroke, and mood disorders.[4] Specifically, in Alzheimer's disease (AD), an overactivity and/or overexpression of GSK-3 plays a central role in the pathology linking all the neuropathological hallmarks described for this devastating disorder such as amyloid deposition, tau hyperphosphorylation, gliosis, and neuronal death.[5] Regarding mood disorders, dysregulation of GSK-3 disrupts neurogenesis and alters behavior.[6] All these evidence point to specific inhibitors of GSK-3 as promising effective drugs for the treatment of these appalling pathologies.[7−9]

Although several protein kinase inhibitors have reached the clinic in the last five years for the treatment of different types of cancer, some important challenges should be overcome in the search and design of protein kinase inhibitors as effective and safe drugs for clinical use.[10] For example, it is very important to look for ATP noncompetitive kinase inhibitors because the human kinome is composed of more than 500 protein kinases that share a high degree of identity in the catalytic site, the ATP binding pocket.[11] Pharmacological therapies of CNS diseases usually are chronic treatments, which require safe and specific drugs permeable through the blood−brain barrier. These two facts probably have detracted some efforts in the development of protein kinases inhibitors for CNS disorders although today some of them are on different preclinical and clinical stages of development.[12]

Regarding GSK-3, most of the inhibitors found so far bind to the ATP site on the enzyme.[13] Only few examples of ATP noncompetitive inhibitors have been reported being the thiadiazolidindione family (TDZD), the first one described and the most advanced in development today.[14] Tideglusib, a TDZD small molecule, is currently in clinical trials phase IIb as a disease modifying drug for severe tauopathies such as AD and paralysis supranuclear palsy.[15] As GSK-3 has the ability to

Received: October 31, 2011
Published: January 18, 2012

phosphorylate primed substrates, small molecules able to bind to substrate recognition site and to partially block the activity of the enzyme over some specific substrates, should be perfect drug candidates for those diseases in which an up-regulation of GSK-3 is involved.[16] Furthermore, they would provide more subtle modulation of kinase activity than simply blocking ATP entrance. This is of utmost importance in terms of GSK-3 inhibition as a therapeutic strategy. Only those inhibitors able to modulate the activity of GSK-3 smoothly, without totally inactivating the enzyme activity, will become valuable clinically relevant drugs.[8] Up to now, only some small peptides have been found to target this region of GSK-3, showing promising preclinical results for CNS disorders.[17] However, their poor pharmacokinetic properties detract the potential pharmacological development.

Since the discovery and synthesis of TDZDs as ATP noncompetitive GSK-3 inhibitors in our laboratory, we have done extensive chemical structure−activity relationship studies in the thiadiazolidindione scaffold by varying both the nature and number of heteroatoms present in the central five-membered ring and the substituents attached to this heterocycle (Figure 1).[18,19] Here, we present our results using the

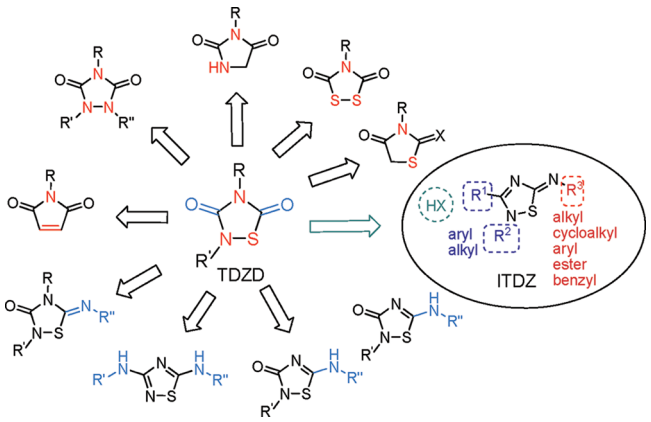

Figure 1. Different heterocyclic families of compounds evaluated in the SAR studies of TDZDs and the new family of ITDZ.

new TDZD-related family of 5-imino-1,2,4-thiadiazoles (ITDZ) where we have kept the thiadiazole ring but we have changed the two carbonyl groups in positions 3 and 5 by different imino and aryl/alkyl moieties. The addition of a C−C bond directly attached to the thiadiazole scaffold confers greater aromaticity and stability to the heterocycle and, as consequence, to the full molecule. This new family of compounds, the ITDZs, resulted to be reversible GSK-3 inhibitors in the low micromolar range, cell permeable compounds able to protect primary neuronal cell cultures from inflammatory insults and to promote differentiation toward a neuronal phenotype of hippocampal adult rat neurospheres. Moreover, ITDZs are substrate competitive GSK-3 inhibitors, being the first small molecules substrate competitive to GSK-3 and a very interesting scaffold to be further developed. Their synthesis, enzymatic and cellular evaluation, as well as molecular modeling studies are presented in this article.

RESULTS AND DISCUSSION

Chemistry. With the aim of obtaining information about chemical structure−biological activity relationship in this new family of ITDZs, different substitutions were made to increase chemical diversity (Figure 1). Mainly, aryl moieties were chosen for diversity in positions directly attached to the heterocyclic framework (R^1 and R^2) but also some alkyl chains were introduced. Substituents at the exocyclic imino nitrogen atom (R^3) were highly varied as the incorporation of this part of the molecule is almost at the end of the synthesis.

ITDZ derivatives were synthesized by oxidative cyclization of imidoiltioureas following previous reported synthetic pathway (Scheme 1).[20,21]

Scheme 1[a]

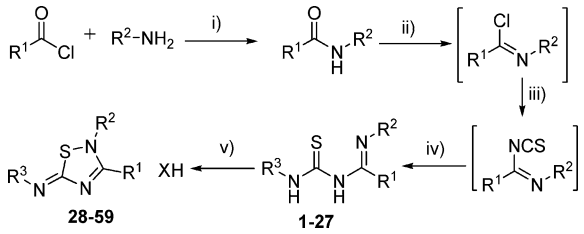

[a]Reagents: (i) Et_3N, AcOEt, rt; (ii) $SOCl_2$, Δ, or PCl_5, toluene, Δ, or oxalyl chloride, lutidine, CH_2Cl_2, 0 °C; (iii) KSCN, acetone, −15 °C; (iv) R^3-NH_2, acetone, 0 °C; (v) Br_2, AcOEt, CH_2Cl_2, from 0 °C to rt, or NCS, CH_2Cl_2, rt, or NCS, CH_2Cl_2, $NaHCO_3$, rt.

The first step of the synthesis consists in the formation of a disubstituted amide in an aprotic solvent and basic medium. Subsequent treatment with thionyl chloride leads to the corresponding imidoyl chlorides used in the next step without further isolation. Sometimes, depending on the nature of R^1 and R^2 substituents, the treatment of the corresponding amide with this chlorinating agent was unsuccessful and, PCl_5 in toluene at reflux temperature was employed (see Table 1). If the substituent R^1 of the amide moiety is an aliphatic residue, oxalyl chloride in lutidine at 0 °C was necessary to use for the preparation of the corresponding imidoyl chloride, after no progression of the reaction with the previous agents. These unstable imidoyl chlorides were treated with potassium thiocyanate to yield the corresponding isothiocyanates, used in the next synthetic step without isolation. Reaction of these isothiocyanates with different primary amines leads to the imidoylthioureas **1**−**27** (Table 1). All these substituted thioureas were isolated and fully characterized by spectroscopic and analytical methods.

Finally, intramolecular oxidative cyclization of imidoylthioureas by treatment with an oxidative agent as bromine or *N*-chloro succinimide (NCS) leads to the corresponding 5-imino-1,2,4-thiadiazole **28**−**58** as hydrobromide or hydrochloride salt (Table 2). Free bases of some of these salts were obtained from the hydrochloride thiadiazoles by treatment with $NaHCO_3$. However, when thiourea **27** was used as starting material, the intramolecular cyclization with the oxidative reagent lead to the fused thiadiazolopyridine heterocyclic compound **59** and not to the expected 5-imino-1,2,4-thiadiazole (Figure 2).

As the analytical data of the great majority of the prepared ITDZ showed the presence of one or two halogen atom in the molecule, to determine which of the three nitrogen atoms were protonated, a careful structural heteronuclear NMR study using different heteronuclear multiple bond correlation (HMBC) sequences for ^1H, ^{13}C, and ^{15}N atoms was done. Analysis of bidimensional spectra of compounds **28**, **29**, and **55** revealed unequivocally that ITDZs are protonated in the nitrogen of the exocyclic imino group. Moreover, conformational studies

dx.doi.org/10.1021/jm201463v | J. Med. Chem. 2012, 55, 1645−1661

Table 1. Chemical Structures and Synthetic Details of the Disubstituted Imidoyltioureas

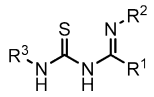

no.	R^1	R^2	R^3	chlorinated reagent used in (ii)	yield (%)
1	Ph	Ph	CH_2-3Pyr	$SOCl_2$	64
2	Ph	Ph	CH_2CO_2Et	$SOCl_2$	40
3	Ph	Ph	CH_2CH_2OH	$SOCl_2$	54
4	Ph	Ph	H	$SOCl_2$	64
5	Ph	Ph	$(CH_2)_4CH_3$	$SOCl_2$	31
6	Ph	Ph	Ph	$SOCl_2$	54
7	Ph	Ph	cyclohex	$SOCl_2$	68
8	Ph	4-OMePh	CH_2-3Pyr	$SOCl_2$	37
9	Ph	4-OMePh	CH_2CO_2Et	$SOCl_2$	30
10	Ph	4-NO_2Ph	CH_2-3Pyr	PCl_5	78
11	Ph	4-NO_2Ph	CH_2CO_2Et	PCl_5	63
12	Ph	4-OMePh	CH_2CH_2OH	$SOCl_2$	33
13	4-OMePh	Ph	CH_2-3Pyr	$SOCl_2$	46
14	4-OMePh	Ph	CH_2CH_2OH	$SOCl_2$	53
15	4-OMePh	Ph	CH_2CO_2Et	$SOCl_2$	28
16	4-OMePh	Ph	$(CH_2)_4CH_3$	$SOCl_2$	47
17	4-OMePh	Ph	Ph	$SOCl_2$	54
18	4-CF_3Ph	Ph	CH_2-3Pyr	$SOCl_2$	40
19	Ph	1-naphthyl	CH_2-3Pyr	PCl_5	58
20	Ph	1-naphthyl	CH_2CH_2OH	PCl_5	24
21	1-naphthyl	Ph	CH_2-3Pyr	PCl_5	59
22	1-naphthyl	Ph	CH_2CH_2OH	PCl_5	49
23	Me	Ph	CH_2-3Pyr	oxalylchloride/lutidine	32
24	$(CH_2)_4CH_3$	Ph	CH_2-3Pyr	oxalylchloride/lutidine	15
25	Ph	Ph	$(CH_2)_2$Morph	$SOCl_2$	70
26	Ph	CH_2Ph	CH_2-3Pyr	PCl_5	31
27	Ph	Ph	2Pyr	$SOCl_2$	84

carried out using different NOE experiments showed that the exocyclic imino group has an *E* configuration in this family of compounds (Table 2). All these spectra are available in the Supporting Information.

Inhibition Evaluation on GSK-3. All the newly prepared compounds (**1**−**59**), both imidoyl thioureas and ITDZs were evaluated in our laboratory as potential GSK-3 inhibitors using a recently well described luminescent technique[22] as a safer nonradioactive assay. While all the imidoyl thioureas **1**−**27** did not show GSK-3 inhibition at the concentration tested (10 μM), all the ITDZs compounds **28**−**58** showed more than 60% of enzymatic inhibition at the same concentration. In all cases, the concentration at which the 50% of inhibition (IC_{50}) is produced was calculated by obtaining values in the low micromolar−submicromolar range (Table 2). These data show that the five-membered 1,2,4-thiadiazole heterocyclic framework is a privileged scaffold for GSK-3 inhibitory activity, a fact previously observed in the TDZDs family.[14,18] A lack of inhibitory activity was observed for compound **59** (14% inhibition at 10 μM) which can be explained because the required 1,2,4-thiadiazole scaffold is not present in the final chemical structure.

The small differences on GSK-3 inhibition values found in this family of compounds do not allow drawing any clear structure activity relationship. However, it is clear that the presence of the 1,2,4-thiadiazole moiety is an important chemical feature for biological activity. To gain insights into the possible reasons for inhibitory activity of this heterocyclic family, we performed a docking study in two steps, first a "*blind/ensemble docking*" and second a "*docking refinement*" (see Experimental Section for details). GSK-3 is an enzyme with a wide conformational space given by the mobility of some relevant portions of the protein such as the "activation loop" or "P-loop", for example. In the case of human GSK-3, several tridimensional structures are present in the Protein Data Bank (PDB),[23] which allow us to see the conformational richness of this protein. To take into account such conformational richness in docking studies ("*ensemble docking*"), we have determined previously three significant structures according to the "P-loop" conformation: 1PYX, 1Q41, and 1Q4L.[24] Furthermore, structures 1I09 and 2JLD were also included to explore better the protein conformational landscape. The docking study was performed over the whole GSK-3 surface (*blind docking*) with compounds **28**−**58** using these different 3D coordinates for GSK-3 structures obtained from PDB. Docking analysis of the best solutions showed the most populated cluster in the substrate binding site, giving us a clue of the preferred location of all ITDZs (Figure 3).

To test the interesting results obtained with the "*blind docking*" study, different kinetic studies were performed. Three different compounds were chosen (**28**, **30**, and **55**) to analyze both the reversibility of the binding and the competition with ATP or with the substrate used in the enzymatic reaction. In our case, we used the small peptide GS-2 similar to skeletal muscle glycogen synthase. In all cases, TDZD-8 was used as reference in these experiments.

First of all, we determined the inhibitory activity on GSK-3 of the three compounds at different preincubation times (Figure

dx.doi.org/10.1021/jm201463v | *J. Med. Chem.* 2012, 55, 1645−1661

Table 2. Chemical Structures, Synthetic Details and Biological Inhibition of GSK-3 of 5-Imino-1,2,4-thiadiazoles (ITDZs)

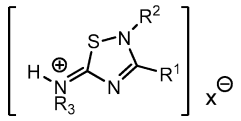

no.	R^1	R^2	R^3	X	oxidative reagent used in (v)	yield (%)	GSK-3 IC_{50} (μM)
28	Ph	Ph	$-CH_2$-3Pyr	2Br	Br_2/AcOEt	64	1.3 ± 0.4
29	Ph	Ph	$-CH_2CO_2Et$	Br	Br_2/AcOEt	64	7.0 ± 1.0
30	Ph	Ph	$-CH_2CH_2OH$	Br	Br_2/AcOEt	30	2.0 ± 0.4
31	Ph	Ph	H	Br	Br_2/AcOEt	30	0.6 ± 0.0
32	Ph	Ph	$-(CH_2)_4CH_3$	Br	Br_2/AcOEt	42	1.4 ± 0.1
33	Ph	Ph	−Ph	Br	Br_2/AcOEt	54	0.9 ± 0.3
34	Ph	Ph	−cyclohex	Br	Br_2/AcOEt	26	2.1 ± 0.3
35	Ph	4-OMePh	$-CH_2$-3Pyr	2Br	Br_2/AcOEt	13	4.1 ± 0.8
36	Ph	4-OMePh	$-CH_2CO_2Et$	Br	Br_2/AcOEt	10	2.0 ± 0.2
37	Ph	4-NO_2Ph	$-CH_2$-3Pyr	2Br	Br_2/AcOEt	13	1.0 ± 0.2
38	Ph	4-NO_2Ph	$-CH_2CO_2Et$	Br	Br_2/AcOEt	64	1.0 ± 0.1
39	Ph	4-OMePh	$-CH_2CH_2OH$	Br	Br_2/AcOEt	10	4.6 ± 0.2
40	4-OMePh	Ph	$-CH_2$-3Pyr	2Br	Br_2/AcOEt	56	1.2 ± 0.1
41	4-OMePh	Ph	$-CH_2CH_2OH$	Br	Br_2/AcOEt	46	1.2 ± 0.4
42	4-OMePh	Ph	$-CH_2CO_2Et$	Br	Br_2/AcOEt	31	0.5 ± 0.0
43	4-OMePh	Ph	$-(CH_2)_4CH_3$	Br	Br_2/AcOEt	42	0.3 ± 0.0
44	4-OMePh	Ph	−Ph	Br	Br_2/AcOEt	15	1.1 ± 0.2
45	4-CF_3Ph	Ph	$-CH_2$-3Pyr	2Br	Br_2/AcOEt	33	1.6 ± 0.3
46	Ph	1-naphthyl	$-CH_2$-3Pyr	2Br	Br_2/AcOEt	80	2.0 ± 0.2
47	Ph	1-naphthyl	$-CH_2CH_2OH$	Br	Br_2/AcOEt	52	0.3 ± 0.0
48	1-naphthyl	Ph	$-CH_2$-3Pyr	2Br	Br_2/AcOEt	64	2.1 ± 0.2
49	1-naphthyl	Ph	$-CH_2CH_2OH$	Br	Br_2/AcOEt	20	0.3 ± 0.0
50	Me	Ph	$-CH_2$-3Pyr	2Br	Br_2/AcOEt	25	0.6 ± 0.0
51	$-(CH_2)_4CH_3$	Ph	$-CH_2$-3Pyr	2Br	Br_2/AcOEt	13	0.8 ± 0.0
52	Ph	Ph	$-CH_2CH_2OH$	Cl	NCS	48	0.6 ± 0.1
53	1-naphthyl	Ph	$-CH_2$-3Pyr	Cl	NCS	32	0.9 ± 0.1
54	4-OMePh	Ph	$-(CH_2)_4CH_3$	Cl	NCS	28	1.1 ± 0.1
55	Ph	Ph	$-(CH_2)_2$Morph	2 Br	Br_2/AcOEt	51	0.9 ± 0.1
56	Ph	Ph	−Ph		NCS	32	2.8 ± 0.4
57	Ph	Ph	$-CH_2CO_2Et$		NCS	65	1.8 ± 0.1
58	Ph	$-CH_2Ph$	$-CH_2$-3Pyr	2 Br	Br_2/AcOEt	8	1.1 ± 0.1

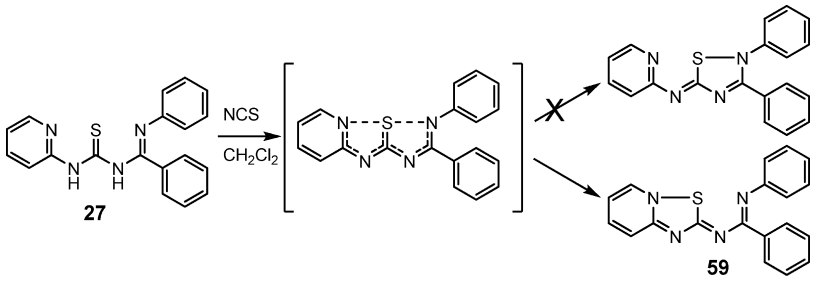

Figure 2. Formation and chemical structure of compound **59**.

4). We used as standard reference three well-known GSK-3 inhibitors with different binding profiles: alsterpaullone, HMK-32, and TDZD-8. Thus, the enzyme inhibition of TDZD-8 increased with preincubation time in the same way of irreversible inhibitors, such as HMK-32 previously determined.[25] However, the inhibition of the ITDZs **28**, **30**, and **55** remained unaltered at different preincubation times, mimicking the behavior of the reversible inhibitor alsterpaullone[25] and other GSK-3 reversible inhibitors.[24] This behavior represents an important difference between TDZD-8 and ITDZs compounds. Although the S−N bond present in the heterocyclic scaffold is able to open in different conditions in both cases, previous studies reported on different substituted 5-imino-1,2,4-thiadiazoles prepared as adenosine antagonist showed a reversible binding to the receptor,[21] which is in agreement with the behavior found here in the binding to GSK-3.

Kinetic experiments varying both ATP (from 1 to 50 μM) and ITDZs concentrations were also performed. Double-reciprocal plotting of the data is depicted in Figure 5. The intercept of the plot in the vertical axis ($1/V$) rises when the ITDZs concentration increases (from 0.4 to 2 μM), whereas the intercept in the horizontal axis ($1/[ATP]$) does not change, meaning that, while the enzyme maximal rate (V_{max}) decreases

dx.doi.org/10.1021/jm201463v | J. Med. Chem. 2012, 55, 1645−1661

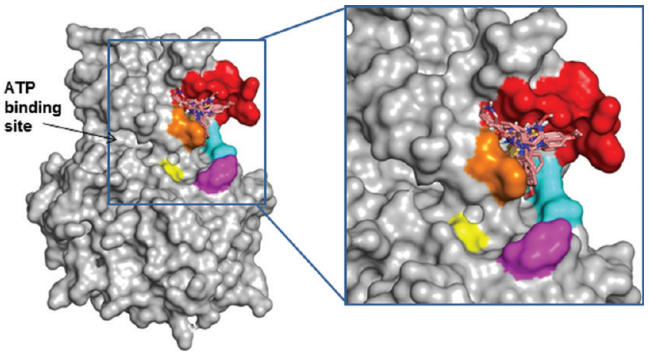

Figure 3. Best solution of the ITDZs docked on GSK-3 surface (PDB code 1Q4L). The inhibitors bind in the substrate pocket of the enzyme. GSK-3 interacting sites with substrates:[13] hydrophobic patch (cyan), F67 (orange), 89−95 loop (red), phosphate binding pocket (blue), D181 (yellow) interacts with the pseudosubstrate.

in the presence of the inhibitor, the Michaelis−Menten constant (K_m) remains unaltered. These results would suggest that derivatives **28**, **30**, and **55** act as noncompetitive inhibitors of ATP binding because an increase in the ATP concentration (from 1 to 50 μM) does not interfere with enzymatic inhibition. The same behavior was previously reported for TDZD-8[14] and others TDZDs,[18] the first ATP noncompetitive GSK-3 inhibitors reported in the literature.

Finally, kinetic experiments were performed also by varying the concentrations of both GS-2 (from 12.5 to 100 μM) and ITDZs inhibitors **28**, **30**, and **55** (0.5, 1, 2, and 2.5 μM, respectively), while the ATP concentration was kept constant (1 μM). Double-reciprocal plotting of the data (Figure 6) suggests that these compounds act as competitive inhibitors of GS-2 binding. These results are in clear contrast with those obtained for TDZD-8 and other TDZDs that do not compete with the substrate.

In summary, collective results here presented reveal that the binding of ITDZs to GSK-3 is reversible, noncompetitive with ATP, and substrate competitive. These data provide the ITDZs as the first small molecules that compete with the primed substrate in GSK-3 inhibition. Until now, only some peptides[16] or the complex natural alkaloid manzamine[26] have been reported as substrate competitive GSK-3 inhibitors. The specific mechanism of inhibition here presented adds great value to these compounds for their potential further development. Probably only ATP noncompetitive modulators of GSK-3 will have an impact in the clinic because a subtle inhibition of GSK-3 is completely necessary to restore the aberrant overactivity found in pathologies without producing serious side effects in healthy tissues.[13]

Binding Mode of ITDZs on GSK-3. Once studied experimentally that the binding of ITDZs to GSK-3 is reversible, noncompetitive with ATP, and substrate competitive, we performed an optimization of the previous blinded docking (“*refine docking*”) with the aim to determine the specific amino acids involved in the binding of ITDZs to GSK-3 and to analyze the driving interactions of these complexes.

The analysis of the activity data (IC_{50} of Table 2) together with our previous docking studies led us to conclude that the inhibition of GSK-3 is mainly due to the 5-imino-1,2,4-thiadiazole scaffold (Figure 7). The main interactions of this privileged framework take place through a hydrogen bond (HB) between the proton of the imino charged group and the backbone oxygen of Phe67 and aromatic S−π interaction between the thiadiazole heterocycle and the aromatic ring of Phe67.

Regarding the different substitution in R^1, R^2, or R^3 and as a general rule, the interaction of these groups with the binding site of GSK-3 is mediated by specific aromatic interactions. In the first place, we focus on substituents in R^1 and R^2. Different chemical moieties introduced in R^1 can interact with Gln89, Asp90, Arg96, or Phe67 depending on their nature. In fact, when a benzene group is attached in such position, as for example in compound **31**, NH−π interactions with the backbone of Asp90 or Gln89's side chain come into play. As

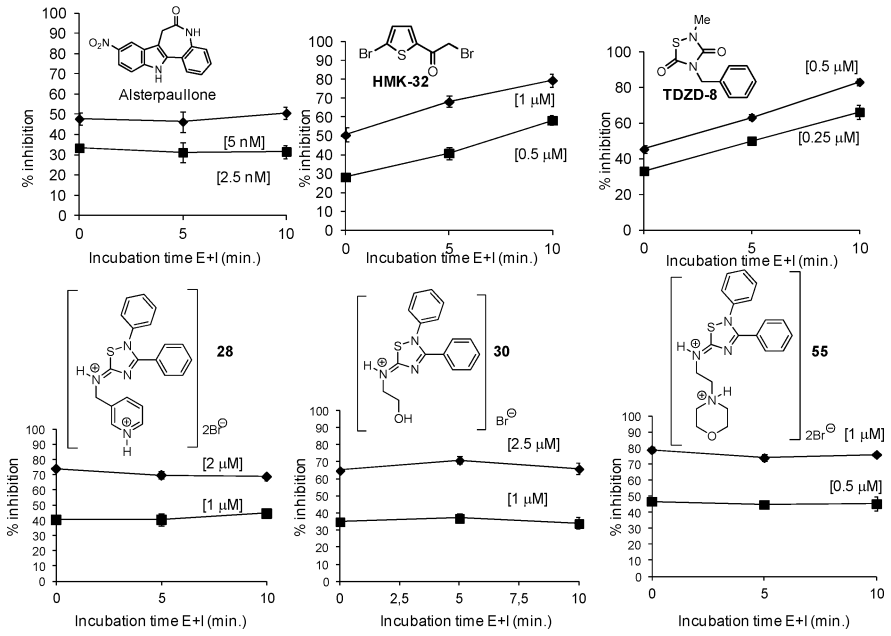

Figure 4. Time dependent GSK-3 inhibition of standard references (alsterpaullone, HMK-32, and TDZD-8) and the new synthesized ITDZs compounds **28**, **30**, and **55**.

dx.doi.org/10.1021/jm201463v | *J. Med. Chem.* 2012, 55, 1645−1661

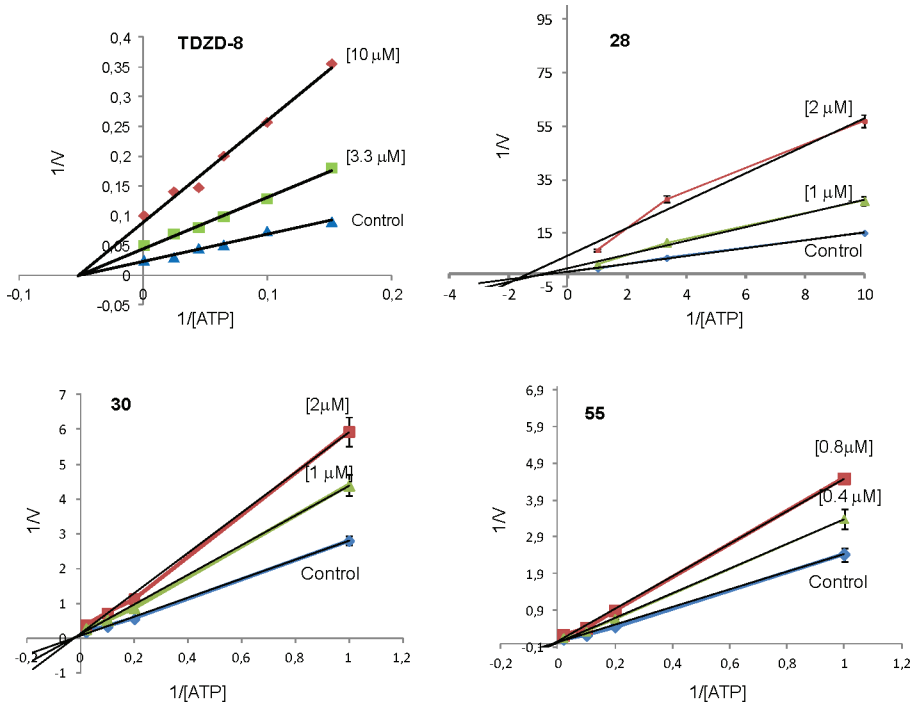

Figure 5. Kinetic data determined for TDZD-8 and the ITDZs derivatives **28**, **30**, and **55**. ATP concentrations in the reaction mixture varied from 1 to 50 μM. Compound concentrations used are depicted in the plot, and the concentration of GS-2 was kept constant at 12.5 μM. Each point is the mean of two different experiments, each one analyzed in duplicate.

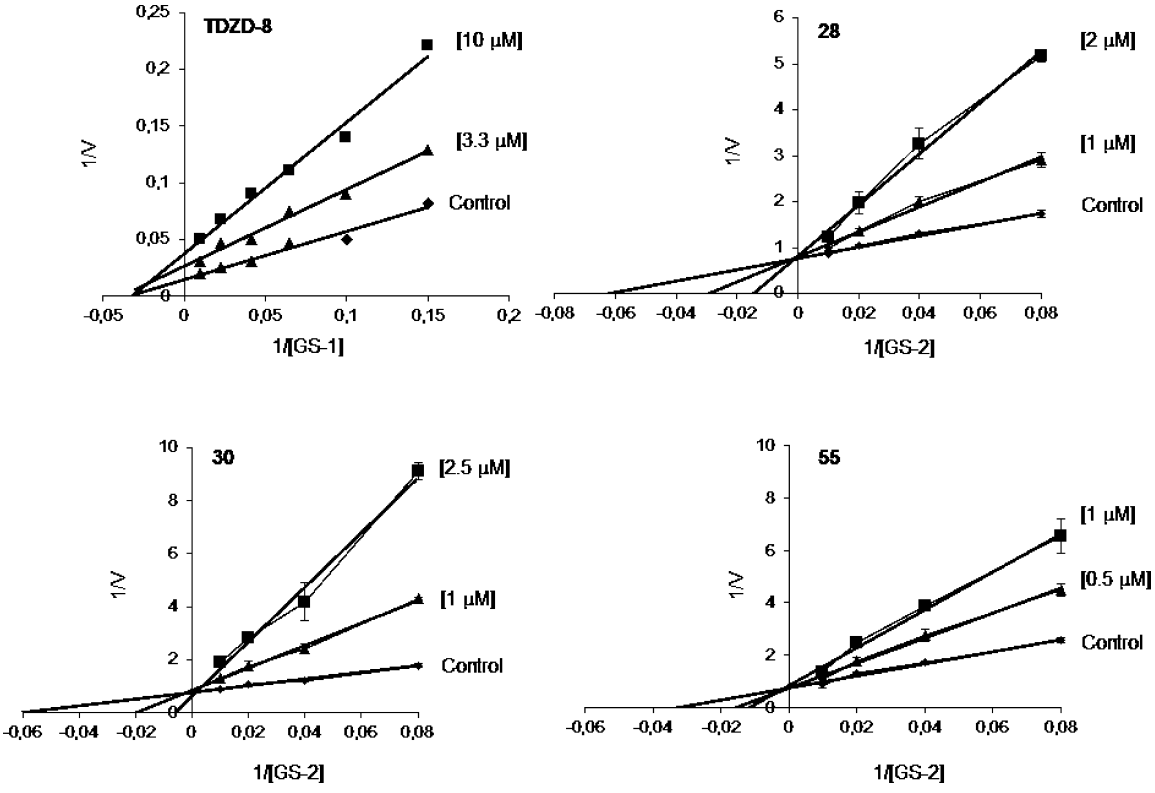

Figure 6. Kinetic data determined for TDZD-8 and the ITDZs derivatives **28**, **30**, and **55**. GS-2 concentrations in the reaction mixture varied from 12.5 to 100 μM. Compound concentrations used are depicted in the plot, and the concentration of ATP was kept constant at 1 μM. Each point is the mean of two different experiments, each one analyzed in duplicate.

it is seen in Figure 8, the benzene ring attached in R^1 is close to the backbone −NH group of Asp90, leading to a NH−π interaction[27] but far from Phe93 which adopts a quite exposed orientation. However, when a Me (compound **50**) or naphthyl group (for example compounds **46**, **48**) replaces the benzene, the ligand in R^1 changes its orientation within the binding site

dx.doi.org/10.1021/jm201463v | J. Med. Chem. 2012, 55, 1645−1661

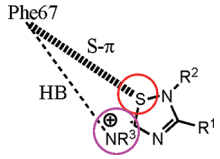

Figure 7. Key structural interactions for the binding of ITDZs to GSK-3.

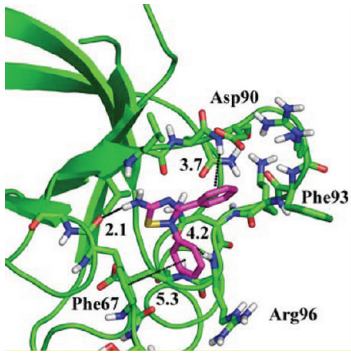

Figure 8. Binding mode of compound **31** against PDB code 1Q4L of GSK-3 showing relevant interactions (distances in angstroms) with nearby residues.

facing such groups toward Phe67's side chain in order, on the one hand, to establish stronger S−π interactions[28] with the thiadiazole heterocycle and the other to favor π−CH_3 and π−π interactions.

On the other hand, substituents introduced in R^2 allow ligands to interact with side chains of Phe67 or Arg96 by means of π−π, cation−aromatic,[29,30] hydrophobic, or electrostatic interactions. Thus, when a benzene is placed in R^2 (compound **31**), the ligand orientation within the binding site tries to optimize a π−π interaction with Phe67 side chain, usually resulting in a "parallel-displaced" orientation and a possible cation−aromatic with Arg96's side chain. The former interaction is perfectly established when a naphthyl group (compound **47**) replaces the benzene in position R^2 as a "face to face" orientation is achieved (Figure 9). On the other hand,

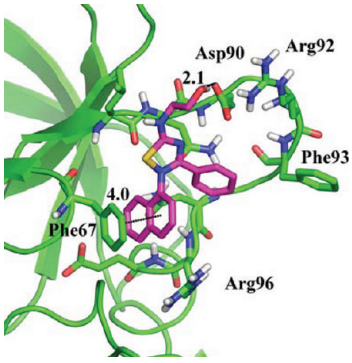

Figure 9. Binding mode of compound **47** against PDB code 1Q4L of GSK-3 showing relevant interactions (distances in Å) with nearby residues.

when a $-NO_2$ group is introduced, a strong electrostatic interaction is established with Arg96's side chain. Finally, when a methoxy group (compound **35**, data not shown) is introduced, a lot of clashes come into play, resulting in a lower activity.

Substituents attached in R^3, allow ligands to interact with residues Phe67, Leu88, and Asp90, depending on the nature of the group attached in such position. Thus, when aliphatic groups are added, the interactions are of hydrophobic kind mainly with the Leu88's side chain. On the contrary, when the introduced groups have donor or acceptors they interact by means of hydrogen bonds with the −NH or ═O backbone groups of residues Leu88 and/or Phe67, respectively. Finally, in the particular case of compounds **50** and **51**, where pyridine moieties or morpholine (compound **55**) are attached to R^3, they interact by means of strong electrostatic interactions with Asp90s side chain (Figure 10).

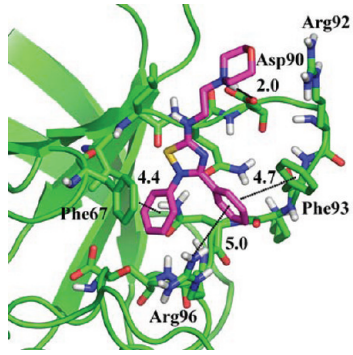

Figure 10. Binding mode of compound **55** against PDB code 1Q4L of GSK-3 showing relevant interactions (distances in Å) with nearby residues.

Cellular Effects of GSK-3 Inhibition. To evaluate the cell permeability of ITDZs inhibitors and their potential use as pharmacological tools and/or leads for drug design, we further explored their neuroprotective activity against inflammatory activation and their neurogenic potential on adult neural stem cells. These two properties are linked to the potential of a new drug for delay or stop the neuronal loss and for increase the endogeneous neurogenesis as a repair mechanism in the damaged brain, which adds great value in compounds designed as new drugs for neurodegenerative disorders.

Neuroprotection. As an overexpression and/or over activity of GSK-3 is involved in the increase of microglia activation in different neurodegenerative diseases leading to the neuronal cell death[31] and it is proved that GSK-3 regulates inflammatory tolerance in astrocytes,[32] we next explored whether these new GSK-3 inhibitors, the ITDZs compounds, are neuroprotective and exert an anti-inflammatory action in different cell-based assays. Thus, we used primary cultures of astrocytes, microglia and neurons treated with lipopolysaccharide (LPS), a potent inflammatory agent, and/or with cell-free supernatant from LPS-activated microglia.

The potential anti-inflammatory activity of the selected GSK-3 inhibitors was first tested by evaluating the production of nitrites from primary cultured glial cells, astrocytes and microglia. Cultures were incubated with the indicated concentrations of the compounds **28**−**30**, **39**, and **52** for 1 h, and then cells were cultured for another 24 h with LPS. When primary astrocytes and microglial cells were stimulated with LPS (Figure 11), we observed a significant induction of nitrite production in the culture medium (3- to 4-fold, respectively), which was significantly decreased by ITDZs treatment.

We next investigated whether these compounds were also effective in protecting neurons from the injury induced by the

dx.doi.org/10.1021/jm201463v | J. Med. Chem. 2012, 55, 1645−1661

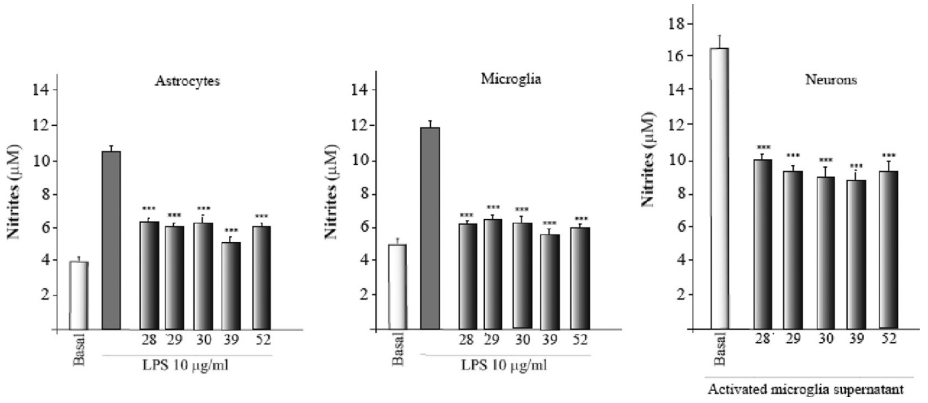

Figure 11. Primary glial cultures, microglia and astrocytes, were treated with lipopolysaccharide (LPS) in the presence or absence of the indicated compounds at different concentrations, and primary neuronal cultures were treated with conditioned medium from LPS-activated microglial cells. Twenty-four hours after exposure to the compounds, the production of nitrites was measured with the Griess reaction.

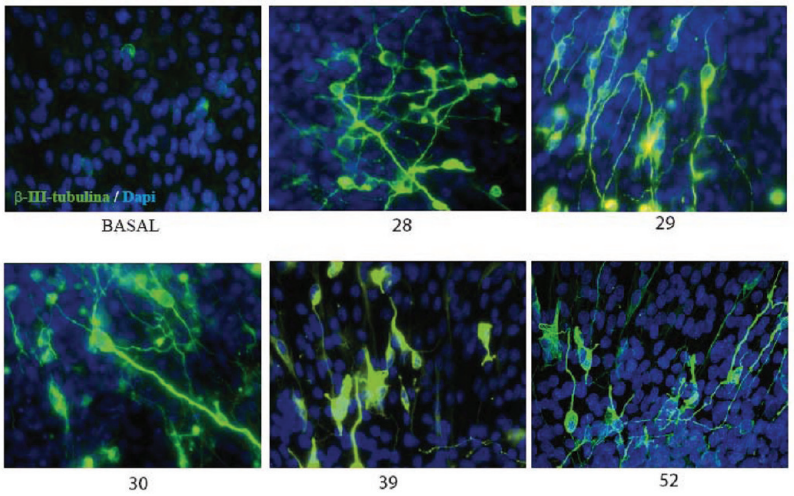

Figure 12. The neural stem cells are isolated from the hippocampus of adult rat brain. The neurospheres are cultivated in the presence or absence of different compounds during a week, after which they are seeded in a poly lysine substrate, fixed, stained anti-β-tubulin antibody, and counterstained with DAPI (blue).

cell-free supernatant from LPS-activated microglia, a cellular model for the damage caused by brain environment in a neurodegenerative disease. As shown in Figure 11, treatment of neuronal cultures with compounds **28**−**30**, **39**, and **52** also resulted in a significant reduction in nitrite production.

Altogether these results indicate that GSK-3 inhibitors, especially those of 5-imino-1,2,4-thiadiazole scaffold, such as derivatives **28**−**30**, **39**, and **52**, are potent anti-inflammatory and neuroprotective agents in primary neural cultures.

Neurogenesis. To evaluate the potential neurogenic effect of the new compounds and to demonstrate their ability to repair brain damage, we used primary neural stem cells obtained from adult rats. Previously, we have demonstrated that neural stem cells expressed GSK-3β when isolated and cultured in vitro to form neurospheres.[33]

Next, we analyzed whether addition of the different ITDZs inhibitors (**28**−**30**, **39**, and **52**) could regulate cell differentiation toward a neuronal phenotype after adhesion of neurospheres.

Neurospheres were allowed to adhere to the substrate and then incubated for 24 h in the absence of EGF and FGF and in the presence or absence of the different ITDZs. As shown in Figure 12, in control cultures only scattered cells stained with β-tubulin (clone Tuj1) were observed. However, the number of β-tubulin positive cells was significantly increased in those cultures treated with the ITDZs compounds **28**−**30**, **39**, and **52**.

Blood−**Brain Barrier Penetration.** Finally, to know some drug-like properties of the new compounds here presented, especially those required for their use in different in vivo diseases models, we determined their ability to cross the blood−brain barrier (BBB) as a key feature to consider these compounds as drug candidates for the potential treatment of CNS diseases.

The complex neural function of the CNS depends on a highly stable environment, enabling proper firing and communication of its neurons.[34] The BBB is a protective system composed by microvascular endothelial cells that prevent the entrance of molecules and other substances from the blood into the brain, keeping the homeostasis of this microenvironment. Lipid soluble molecules are able to penetrate through the barrier relatively easily via the lipid membranes of the cells. In contrast, water-soluble molecules (e.g., ions) are unable to transverse the barrier without the use of specialized carrier-mediated transport mechanisms. Determination of BBB penetration at early stages during drug

dx.doi.org/10.1021/jm201463v | J. Med. Chem. 2012, 55, 1645−1661

discovery phases is important to obtain the best candidate for further development. Parallel artificial membrane permeability assay (PAMPA) is a high throughput technique developed to predict passive permeability through biological membranes. To explore the capacity of the ITDZs synthesized to penetrate into the brain, we used the PAMPA-BBB method described by Di et al,[35] which employed a brain lipid porcine membrane. First, an assay validation was made comparing the reported permeabilities (*Pe*) values of commercial drugs with the experimental data obtained by employing this methodology (see Supporting Information). The in vitro permeabilities (*Pe*) of commercial drugs through lipid membrane extract together with ITDZs compounds were determined and described in Table 3.

Table 3. Permeability (*Pe* 10^{-6} cm s^{-1}) in the PAMPA-BBB Assay for 10 Commercial Drugs (Used in the Experiment Validation) and Different ITDZs Compounds with Their Predictive Penetration in the CNS[a]

compd	bibl[b]	*Pe* (10^{-6} cm s^{-1})[c]	BBB prediction
atenolol	0.8	0.5 ± 0.3	
caffeine	1.3	1.6 ± 0.2	
desipramine	12	14.9 ± 1.1	
enoxacin	0.9	0.9 ± 0.3	
hydrocortisone	1.9	2.2 ± 0.3	
ofloxacin	0.8	1.2 ± 0.2	
piroxicam	2.5	1.7 ± 0.3	
promazine	8.8	8.9 ± 1.0	
testosterone	17	15.9 ± 1.1	
verapamil	16	16.0 ± 0.8	
28		10.7 ± 0.3	CNS +
29		6.2 ± 0.4	CNS +
30		15.8 ± 0.4	CNS +[37]
31		9.1 ± 0.8	CNS +[38]
33		not soluble	
34		not soluble	
35		6.3 ± 0.3	CNS +
36		4.4 ± 0.4	CNS +[38]
39		13.4 ± 0.9	CNS +[38]
40		4.8 ± 0.4	CNS +
41		13.7 ± 0.8	CNS +
42		4.0 ± 0.1	CNS +/ CNS −
44		not soluble	
45		not soluble	
49		10.2 ± 0.6	CNS +
50		5.3 ± 0.5	CNS +
52		13.6 ± 0.4	CNS +[38]
54[d]		8.5 ± 0.5	CNS +
55[d]		7.2 ± 0.8	CNS +
56		not soluble	

[a]PBS:DMSO (95:5) was used as solvent. [b]Reference 35. [c]Data are the mean ± SD of 3 independent experiments. [d]PBS:EtOH (70:30) was used as solvent.

A good correlation between experimental-described values was obtained *Pe*(exp) = 1.0125 (bibl) + 0.1227 (R^2 = 0.974). From this equation and following the pattern established in the literature for BBB permeation prediction,[36] we could classify compounds as CNS + when they present a permeability >4.17 × 10^{-6} cm s^{-1}. On the basis of these results, we evaluated the ability to cross the BBB of 20 different ITDZs. Results obtained show that a great number of compounds, namely **28**−**31**, **33**−**36**, **39**−**42**, **44**−**45**, **49**-**50**, **52**, and **54**−**56**, are able to cross the BBB by passive permeation, thus they can be used in further steps development involving animal models. Compounds **33**−**34**, **44**−**45**, and **56** precipitate under these experimental conditions.

CONCLUSIONS

The search for allosteric inhibitors of protein kinases involved in human diseases is one of the hot topics in current medicinal chemistry. The pivotal role of GSK-3 in many neurological disorders, including neurodegenerative diseases, is well-documented, being one of the current challenges the search for ATP noncompetitive modulators of GSK-3.

Following the optimization process in the TDZD scaffold, we here described the ITDZs derivatives as the first small molecules reported to be substrate competitive GSK-3 inhibitors. These compounds are cell permeable, showing a reduction of the inflammatory activation on different primary neural cell cultures and the ability to differentiate neural stem cells to mature neurons. Moreover, they are able to penetrate the CNS in an in vitro model, being good candidates for further in vivo studies. In fact, some of them are in progress, showing good preliminary results regarding both neuroprotective and neurogenic potential. Overall, the new allosteric GSK-3 inhibitors here reported might have a great impact in therapy not only for the potential modification of the course of neurodegeneration decreasing neuronal injury but also for the potential of repairing the damaged brain. Collectively, our findings indicate that ITDZs might be of relevant therapeutic importance in the treatment of neurodegenerative diseases.

EXPERIMENTAL SECTION

General Chemical Methods. Substrates were either purchased from commercial sources or used without further purification. Melting points were determined with a Mettler Toledo MP70 apparatus and are uncorrected. Flash column chromatography was carried out at medium pressure using silica gel (E. Merck, grade 60, particle size 0.040−0.063 mm, 230−240 mesh ASTM) with the indicated solvent as eluent. Compounds were detected with UV light (254 nm). ^{1}H NMR spectra were obtained on a Bruker AVANCE-300 spectrometer working at 300 MHz and on the Varian INNOVA-300 operating at 300 MHz. Typical spectral parameters: spectral width 10 ppm, pulse width 9 μs (57°), data size 32 K. Description of signals: s = singlet, bs = broad singlet, d = doublet, t = triplet, q = quartet, m = multiplet, dd = doublet of doublet, ddd = doublet of dd, dt = doublet of triplets. ^{13}C NMR experiments were carried out on the Bruker AVANCE-300 spectrometer operating at 75 MHz and on the Varian INNOVA-400 or Varian MERCURY-400, both operating at 100 MHz. The acquisiton parameters: spectral width 16 kHz, acquisition time 0.99 s, pulse width 9 μs (57°), data size 32 K. ^{15}N NMR experiments were carried out on the Varian Unity-500 operating at 500 MHz. Chemical shifts are reported in values (ppm) relative to internal Me_4Si, and *J* values are reported in hertz. Elemental analyses were performed by the analytical department at CENQUIOR (CSIC), and the results obtained were within ±0.4% of the theoretical values. Mass spectra were obtained by electronic impact in a Hewlett-Packard 5973 spectrophotometer. HPLC analyses for compounds **1**−**27** were performed on a Waters 6000 instrument, with UV detector (214−254 nm), using different columns; μ Alliance Waters 2690 equipment with a UV detector photodiode array Waters 2996 with MS detector MicromassZQ (Waters) positive electrospray, using the Sunfire column C18, 3.5 μm (50 mm × 4.6 mm) and acetonitrile (0.08% formic acid) and MilliQ water (0.1% formic acid) as mobile phase in a 10 min run from 10% to 100% acetonitrile gradient at a flow rate of 0.25 mL/min. All compounds are >95% pure by HPLC analyses.

General Procedure for Imidoyl Chloride Synthesis via Thionyl Chloride.[20,21] A mixture of the corresponding amide (1

dx.doi.org/10.1021/jm201463v | J. Med. Chem. 2012, 55, 1645−1661

equiv) with thionyl chloride (1.2 equiv) was heated at 135 °C for 4 h. Afterward, the resulting mixture was allowed to cool to room temperature, dichloromethane was added, and the solvent and excess of thionyl chloride were evaporated under reduce pressure. The imidoyl chlorides obtained were used in the next step of the synthesis without further purification.

General Procedure for Imidoyl Chloride Synthesis via Phosphorus Pentachloride.[39] An equimolar mixture of the corresponding amide with phosphorus pentachloride was heated in toluene under reflux for 4 h. Afterward, the resulting mixture was allowed to cool to room temperature, the solids formed were filtered off, and the solvent was evaporated under reduced pressure. The products obtained were used in the next step of the synthesis without further purification.

General Procedure for Imidoyl Chloride Synthesis via Phosphorus Oxalyl Chloride.[40] Over a solution of the corresponding amide (1 equiv) in dichloromethane at 0 °C, 2,6-lutidine (1.66 equiv) was added. Afterward, oxalyl chloride (1 equiv) was slowly added and the reaction mixture was left for 30 min. After evaporation of the solvent under reduced pressure, the product obtained was used in the next step of the synthesis without further purification.

General Procedure for Imidoylthioureas Synthesis.[20,21] Over a solution of the corresponding imidoyl chloride (1 equiv) in anhydrous acetone at −15 °C, and under inert conditions, a solution of potassium thyocianate (1.1 equiv) in acetone was slowly added. After the addition was completed, the mixture was allowed to reach 0 °C, filtered through a plug of Celite, and then the primary amine (1.1 equiv) was added at 0 °C. (For the imidoylthioureas **2**, **9**, **11**, and**15**, the corresponding amine was purchased as hydrochloride salt, therefore it was previously stirred with sodium bicarbonate (3 equiv) for 15 min at room temperature.) The resulting reaction mixture was stirred at room temperature for 12−24 h. The solvent was then removed under reduced pressure, and the remaining solid was purified with several methanol washes or flash column chromatography.

3-(*N*-Phenylbenzimidoyl)-1-(3-pyridylmethyl)thiourea (1). *N*-Phenylbenzimidoyl chloride (0.37 g, 1.72 mmol), potassium thyocianate (0.182 g, 1.89 mmol), and 3-(aminomethyl)pyridine (0.190 mL, 1.89 mmol). The crude product was purified with several methanol washes to afford a yellow solid (0.366 g, 64%); mp 146−147 °C. ^{1}H NMR ($CDCl_3$) δ 12.48 (s, 1H), 8.68 (s, 1H), 8.55 (d, 1H, J = 4.2 Hz), 8.15 (s, 1H) 7.84 (dd, 1H, J = 1.7 Hz, 7.68 Hz), 7.68−6.94 (m, 9H), 6.64 (d, 2H, J = 6.8 Hz), 5.0 (d, 2H, J = 5.0 Hz). ^{13}C NMR ($CDCl_3$) δ 181.2, 155.7, 149.0, 148.7, 146.2, 135.7, 132.9, 131.9, 130.7, 128.8, 128.1, 123.9, 123.6, 122.3, 46.7. HPLC: purity >99%, rt = 3.65 min. MS (ESI+): 347 [M + H].

1-Ethoxycarbonylmethyl-3-(*N*-phenylbenzimidoyl)thiourea (2). *N*-Phenylbenzimidoyl chloride (0.355 g, 1.65 mmol) and potassium thyocianate (0.176 g, 1.81 mmol). Ethyl aminoacetate hydrochloride (0.193 g, 1.81 mmol) was used after being stirred in anhydrous acetone for 15 min at room temperature with sodium bicarbonate (0.456 g, 5.43 mmol). The crude product was purified with several methanol washes to afford a pale-orange solid (225 mg, 40%); mp 151−152 °C. ^{1}H NMR ($CDCl_3$) δ 12.46 (s, 1H), 8.08 (s, 1H), 7.34−6.93 (m, 8H), 6.70 (d, 2H, J = 7.5 Hz), 4.50 (d, 2H, J = 4.3 Hz), 4.23 (q, 2H, J = 7.2 Hz), 1.26 (t, 3H, J = 7.2 Hz). ^{13}C NMR ($CDCl_3$) δ 180.7, 168.7, 155.2, 132.0, 130.6, 130.5, 129.1, 128.8, 128.8, 128.0, 124.0, 122.4, 61.6, 47.5, 14.1. HPLC: purity >99%, rt = 4.97 min. MS (ESI+): 342 [M + H].

1-(2-Hydroxyethyl)-3-(*N*-phenylbenzimidoyl)thiourea (3). *N*-Phenylbenzimidoyl chloride (0.643 g, 2.98 mmol), potassium thyocianate (0.317 g, 3.26 mmol), and 2-aminoethanol (0.196 mL, 3.26 mmol). The crude product was purified with several methanol washes to afford a pale-yellow solid (481 mg, 54%); mp 144−145 °C. ^{1}H NMR ($CDCl_3$) δ 12.24 (s, 1H), 8.09 (s), 7.37−6.91 (m, 8H), 6.68 (d, 2H, J = 7.5 Hz), 3.93 (s, 4H), 2.24 (bs, 1H). ^{13}C NMR ($CDCl_3$) δ 181.1, 155.6, 146.5, 132.1, 130.7, 130.5, 129.4, 129.1, 128.8, 128.9, 128.3, 128.2, 123.9, 122.4, 61.6, 47.7. HPLC: purity 97%, rt = 3.92 min. MS (ESI+): 300 [M + H].

1-(*N*-Phenylbenzimidoyl)thiourea (4). *N*-Phenylbenzimidoyl chloride (1.68 g, 7.8 mmol), potassium thyocianate (0.835 g, 8.6 mmol), and 30% aqueous ammonia solution (663 mL, 8.6 mmol). The crude product was purified with several methanol washes to afford a white solid (1.2 g, 64%); mp 168−169 °C (lit.[41] 166−167 °C). ^{1}H NMR ($CDCl_3$) δ 11.15 (s, 1H), 8.05 (s, 1H), 7.47−6.74 (m, 8H), 6.61 (d, J = 7.4 Hz, 2H), 1.54 (s, 1H). ^{13}C NMR ($CDCl_3$) δ 182.8, 155.5, 147.0, 132.3, 131.2, 129.8, 129.4, 129.3, 128.5, 124.4, 122.7. HPLC: purity 95%, rt = 4.53 min. MS (ESI+) 256 [M + H].

1-Pentyl-3-(*N*-phenylbenzimidoyl)thiourea (5). *N*-Phenylbenzimidoyl chloride (1.68 g, 7.8 mmol), potassium thyocianate (0.835 g, 8.6 mmol), and pentylamine (0.995 mL, 8.6 mmol). The crude product was purified with several methanol washes to afford a brown solid (785 mg, 31%); mp 157−158 °C. ^{1}H NMR ($CDCl_3$) δ 11.99 (s, 1H), 8.00 (s, 1H), 7.41−6.92 (m, 8H), 6.68 (d, 2H, J = 7.5 Hz) 3.71 (td, J = 7.1 Hz; 5.5 Hz; 2H), 1.71 (q, J = 7.5 Hz; 2H), 1.47−1.28 (m, 4H), 0.90 (t, J = 7.0 Hz; 3H). ^{13}C NMR ($CDCl_3$) δ 179.8, 155.6, 146.6, 132.1, 130.5, 128.7, 128.7, 128.1, 123.7, 122.3, 45.9, 29.2, 28.0, 22.3, 13.9. HPLC: purity >99%, rt = 5.91 min. MS (ESI+): 326 [M + H].

1-Phenyl-3-(*N*-phenylbenzimidoyl)thiourea (6). *N*-Phenylbenzimidoyl chloride (1.68 g, 7.8 mmol), potassium thyocianate (0.835 g, 8.6 mmol), and aniline (0.783 mL, 8.6 mmol). The crude product was purified with several methanol washes to afford a yellow solid (1.45 g, 54%); mp 143−144 °C (lit.[42] 141−142 °C). ^{1}H NMR ($CDCl_3$) δ 14.09 (s, 1H), 8.15 (s, 1H), 8.0−7.0 (m, 13H) 6.75 (d, J = 7.5 Hz; 2H). ^{13}C NMR ($CDCl_3$) δ 178.8, 155.8, 146.0, 138.2, 132.0, 130.7, 129.0, 128.9, 128.9, 128.2, 126.5, 124.1, 124.0, 122.4. HPLC: purity 95%, rt = 5.26 min. MS (ESI+): 332 [M + H].

1-Cyclohexyl-3-(*N*-phenylbenzimidoyl)thiourea (7). *N*-Phenylbenzimidoyl chloride (1.33 g, 6.2 mmol), potassium thyocianate (0.660 g, 6.8 mmol), and cyclohexylamine (0.778 mL, 6.8 mmol) The crude product was purified with several methanol washes to afford a gray solid (1.42 g, 68%); mp 159−160 °C (lit.[43] 159 °C). ^{1}H NMR ($CDCl_3$) δ 12.08 (s, 1H), 7.91 (s, 1H), 7.33−6.86 (m, 8H), 6.67 (d, J = 7.3 Hz, 2H), 4.33 (m, 1H), 2.11−2.03 (m, 2H), 1.69 (m, 2H), 1.58 (m, 2H), 1.53−1.37 (m, 2H), 1.28 (m, 2H). ^{13}C NMR ($CDCl_3$) δ 178.5, 155.6, 146.6, 132.3, 130.5, 128.7, 128.7, 128.0, 123.8, 122.4, 54.1, 31.8, 31.0, 25.5, 24.3. HPLC: purity 96%, rt = 5.32 min. MS (ESI +): 338 [M + H].

3-(*N*-4-Methoxyphenylbenzimidoyl)-1-(3-pyridylmethyl)-thiourea (8). *N*-(4-Methoxyphenyl)benzimidoyl chloride (1.08 g, 4.4 mmol), potassium thyocianate (0.500 g, 5.15 mmol), and 3-(aminomethyl)pyridine (0.521 mL, 5.15 mmol). The crude product was purified with several methanol washes to afford a yellow solid (612 mg, 37%); mp 142−143 °C. ^{1}H NMR ($CDCl_3$) δ 12.53 (s, 1H), 8.59 (s, 1H), 8.48 (dd, J = 4.8 Hz, 1.4 Hz, 1H), 8.05 (s, 1H), 7.73 (d, J = 7.7 Hz, 1H), 7.37−7.09 (m, 6H), 6.58 (d, J = 8.5 Hz, 2H), 6.47 (d, J = 8.2, 2H), 4.92 (d, J = 4.6 Hz, 2H), 3.64 (s, 3H). ^{13}C NMR ($CDCl_3$) δ 181.6, 156.7, 155.9, 149.6, 149.4, 139.7, 136.1, 133.3, 132.6, 131.1, 129.3, 128.5, 124.0, 123.8, 114.5, 55.7, 47.2. HPLC: purity 98.6%, rt = 2.75 min. MS (ESI+): 377 [M + H].

1-Ethoxycarbonylmethyl-3-(*N*-4-methoxyphenylbenzymidoyl)thiourea (9). *N*-(4-Methoxyphenyl)benzimidoyl chloride (1.08 g, 4.4 mmol) and potassium thyocianate (0.500 g, 5.15 mmol). Ethyl aminoacetate hydrochloride (0.720 g, 5.15 mmol) was used after stirred in anhydrous acetone for 15 min at room temperature with sodium bicarbonate (1.30 g, 15.45 mmol). The crude product was purified with several methanol washes to afford a orange solid (489 mg, 30%); mp 146−147 °C. ^{1}H NMR ($CDCl_3$) δ 12.54 (s, 1H), 7.97 (s, 1H), 7.57−7.02 (m, 5H), 6.59 (s, 4H), 4.45 (s, 2H), 4.19 (q, J = 7.1 Hz, 2H), 3.65 (s, 3H), 1.22 (t, J = 7.1 Hz, 3H). ^{13}C NMR ($CDCl_3$) δ 181.2, 169.1, 156.7, 155.3, 139.7, 132.7, 130.9, 129.3, 128.4, 124.0, 114.4, 62.0, 55.8, 47.9, 14.6. HPLC: purity 97%, rt = 4.84 min. MS (ESI+): 372 [M + H].

3-(*N*-4-Nitrophenylbenzimidoyl)-1-(3-pyridylmethyl)-thiourea (10). *N*-(4-Nitrophenyl)benzimidoyl chloride (1.144 g, 4.12 mmol), potassium thyocianate (0.730 g, 4.53 mmol), and 3-(aminomethyl)pyridine (0.460 mL, 4.53 mmol). The crude product

was purified with several methanol washes to afford a yellow solid (1.256 g, 78%); mp 179−180 °C. ^{1}H NMR ($CDCl_3$) δ 11.95 (s, 1H), 8.71 (s, 1H), 8.59 (d, J = 4.3 Hz, 1H), 8.24 (s, 1H), 8.02 (d, J = 8.9 Hz, 1H), 7.95 (d, J = 8.1 Hz, 1H), 7.51−7.17 (m, 7H), 6.77 (d, J = 8.8 Hz, 2H), 5.04 (d, J = 5.5 Hz, 2H). ^{13}C NMR ($CDCl_3$) δ 177.4, 167.4, 160.0, 131.5, 129.3, 128.0, 124.8, 123.0, 29.7. HPLC: purity 95.1%, rt = 3.37 min. MS (ESI+): 392 [M + H].

1-Ethoxycarbonylmethyl-3-(*N*-4-nitrophenylbenzimidoyl)-thiourea (11). *N*-(4-Nitrophenyl)benzimidoyl chloride (1.144 g, 4.12 mmol) and potassium thyocianate (0.730 g, 4.53 mmol). Ethyl aminoacetate hydrochloride (0.630 g, 4.53 mmol) was used after being stirred in anhydrous acetone for 15 min at room temperature with sodium bicarbonate (1.14 g, 13.6 mmol). The crude product was purified with several methanol washes to afford a pale-yellow solid (636 mg, 63%); mp 189−190 °C. ^{1}H NMR ($CDCl_3$) δ 12.00 (s, 1H), 8.27 (s, 1H), 8.04 (d, J = 8.9 Hz, 2H), 7.57−7.12 (m, 5H), 6.84 (d, J = 8.9 Hz, 2H), 4.50 (d, J = 4.7 Hz, 2H), 4.25 (q, J = 7.1 Hz, 2H), 1.28 (t, J = 7.1 Hz, 3H). ^{13}C NMR ($CDCl_3$) δ 180.2, 168.5, 156.1, 144.0, 131.4, 131.0, 129.2, 128.0, 124.7, 123.0, 61.8, 47.6, 14.1. HPLC: purity >99%, rt = 5.13 min. MS (ESI+): 387 [M + H].

1-(2-Hydroxyethyl)-3-(*N*-4-methoxyphenylbenzimidoyl)-thiourea (12). *N*-(4-Methoxyphenyl)benzimidoyl chloride (1.150 g, 4.68 mmol), potassium thyocianate (0.500 g, 5.15 mmol), and 2-aminoethanol (0.310 mL, 5.15 mmol). The crude product was purified with several methanol washes to afford a white solid (508 mg, 33%); mp 141−142 °C. ^{1}H NMR ($CDCl_3$) δ 12.39 (s, 1H), 8.05 (s, 1H), 7.35 (m, 5H), 6.70 (m, 4H), 3.98 (s, 4H), 3.76 (s, 3H), 2.20 (s, 1H). ^{13}C NMR ($CDCl_3$) δ 181.6, 155.7, 139.9, 130.92, 129.3, 128.5, 123.9, 114.5, 62.2, 55.8, 48.1, 181.2, 169.1, 156.7, 155.3, 139.7, 132.7, 130.9, 129.3, 128.4, 124.0, 114.4, 62.0, 55.8, 47.9. HPLC: purity >99%, rt = 3.85 min. MS (ESI+): 330 [M + H].

3-(*N*-Phenyl-4-methoxyphenylacetimidoyl)-1-(3-pyridylmethyl)-thiourea (13). *N*-Phenyl-(4-methoxypheny)acetimidoyl chloride (1.078 g, 4.4 mmol), potassium thyocianate (0.470 mg, 4.84 mmol), and 3-(aminomethyl)pyridine (0.490 mL, 4.84 mmol). The crude product was purified with several methanol washes to afford a gray solid (761 mg, 46%); mp 175−176 °C. ^{1}H NMR ($CDCl_3$) δ 12.45 (s, 1H), 8.59 (s, 1H), 8.51 (s, 1H), 8.04 (s, 1H), 7.77−7.61 (m, 1H), 7.25−6.43 (m, 10H), 4.92 (d, J = 5.4 Hz, 2H), 3.71 (s, 3H). ^{13}C NMR ($CDCl_3$) δ 181.4, 161.1, 155.4, 149.0, 148.7, 135.8, 129.8, 128.8, 123.6, 122.4, 114.2, 55.3, 46.7. HPLC: purity 96%, rt = 2.89 min. MS (ESI+): 377 [M + H].

1-(2-Hydroxyethyl)-3-(*N*-phenyl-4-methoxyphenylacetimidoyl)thiourea (14). *N*-Phenyl-(4-methoxyphenyl)acetimidoyl chloride (1.078 g, 4.4 mmol), potassium thyocianate (0.470 g, 4.84 mmol), and 2-aminoethanol (0.290 mL, 4.84 mmol). The crude product was purified by flash chromatography (CH_2Cl_2:MeOH 80:1) to afford a white solid (767 mg, 53%); mp 117−119 °C. ^{1}H NMR ($CDCl_3$) δ 12.28 (s, 1H), 8.05 (s, 1H), 7.35−6.57 (m, 9H), 3.93 (m, 4H), 3.77 (s, 3H). ^{13}C NMR ($CDCl_3$) δ 181.7, 161.5, 155.6, 147.1, 130.3, 129.2, 124.5, 124.1, 122.8, 114.5, 62.2, 55.7, 48.09. HPLC: purity 97%, rt = 3.83 min. MS (ESI+): 330 [M + H].

1-Ethoxycarbonylmethyl-3-(*N*-phenyl-4-methoxyphenylacetimidoyl)thiourea (15). *N*-Phenyl-4-methoxyphenylacetimidoyl chloride (1.078 g, 4.4 mmol) and potassium thyocianate (0.470 g, 4.84 mmol). Ethyl aminoacetate hydrochloride (0.675 g, 4.84 mmol) was used after being stirred in anhydrous acetone for 15 min at room temperature with sodium bicarbonate (1.219 g, 14.52 mmol). The crude product was purified by flash chromatography (AcOEt/hexane 1:1) to afford a white solid (457 mg, 28%); mp 120−121 °C. ^{1}H NMR ($CDCl_3$) δ 12.52 (s, 1H), 8.09 (s, 1H), 7.38−6.59 (m, 9H), 4.51 (d, J = 4.8 Hz, 2H), 4.24 (q, J = 7.1 Hz, 2H), 3.77 (s, 3H), 1.27 (t, J = 7.2 Hz, 3H). ^{13}C NMR ($CDCl_3$) δ 181.1, 168.8, 161.3, 155.2, 146.8, 130.1, 129.0, 124.2, 124.0, 122.7, 114.4, 61.8, 55.6, 47.7, 14.4. HPLC: purity 96%, rt = 5.00 min. MS (ESI+): 372 [M + H].

1-Pentyl-3-(*N*-phenyl-4-methoxyphenylacetimidoyl)-thiourea (16). *N*-Phenyl-4-methoxyphenylacetimidoyl chloride (1.163 g, 4.75 mmol), potassium thyocianate (0.510 mg, 5.2 mmol), and pentylamine (0.370 mL, 5.2 mmol). The crude product was purified with several methanol washes to afford a brown solid (792 mg, 47%); mp 125−126 °C. ^{1}H NMR ($CDCl_3$) δ 11.98 (s, 1H), 7.99 (s, 1H), 7.27−6.55 (m, 9H), 3.69 (s, 3H), 3.62 (m, 2H), 1.71−1.57 (m, 2H), 1.29 (d, J = 3.3 Hz, 4H), 0.81 (t, J = 6.9 Hz, 3H). ^{13}C NMR ($CDCl_3$) δ 180.4, 161.4, 155.8, 147.3, 130.3, 129.2, 124.6, 124.0, 122.8, 114.8, 114.5, 55.7, 46.2, 31.3, 29.6, 28.5, 22.7, 14.4. HPLC: purity >99%, rt = 5.88 min. MS (ESI+): 356 [M + H].

1-Phenyl-3-(*N*-phenyl-4-methoxyphenylacetimidoyl)-thiourea (17). *N*-Phenyl-4-methoxyphenylacetimidoyl chloride (1.163 g, 4.75 mmol), potassium thyocianate (0.510 g, 5.2 mmol), and aniline (0.470 mL, 5.2 mmol). The crude product was purified with several methanol washes to afford a yellow solid (928 mg, 54%); mp 129−130 °C. (lit.[43] 126 °C). ^{1}H NMR ($CDCl_3$) δ 14.19 (s, 1H), 8.19 (s, 1H), 7.78 (s, 4H), 7.61−6.54 (m, 10H), 3.83 (s, 3H). ^{13}C NMR ($CDCl_3$) δ 179.2, 161.6, 156.0, 146.8, 138.8, 130.3, 129.3, 129.2, 126.8, 124.4, 124.4, 122.9, 114.6, 55.8. HPLC: purity 99%, rt = 5.42 min. MS (ESI+): 362 [M + H].

3-(*N*-Phenyl-4-trifluoromethylphenylacetimidoyl)-1-(3-pyridylmethyl)thiourea (18). *N*-Phenyl-4-trifluoromethylphenylacetimidoyl chloride (0.580 g, 2.05 mmol), potassium thyocianate (0.220 g, 2.26 mmol), and 3-(aminomethyl)pyridine (0.230 mL, 2.26 mmol). The crude product was purified with several methanol washes to afford a white solid (339 mg, 40%); mp 165−166 °C. ^{1}H NMR ($CDCl_3$) δ 12.32 (s, 1H), 8.68 (s, 1H), 8.54 (d, J = 4.9 Hz, 1H), 8.29 (s, 1H), 7.81 (d, J = 7.9 Hz, 1H), 7.60−6.81 (m, 8H), 6.63 (s, 2H), 4.98 (d, J = 5.1 Hz, 2H). ^{13}C NMR ($CDCl_3$) δ 181.3, 149.0, 148.8, 136.3, 133.2, 129.3, 128.9, 126.1, 124.7, 123.9, 122.4, 47.0. HPLC: purity >99%, rt = 3.83 min. MS (ESI+): 415 [M + H].

3-(*N*-1-Naphthylbenzimidoyl)-1-(3-pyridylmethyl)thiourea (19). *N*-Naphthyl-benzimidoyl chloride (1.940 g, 4.9 mmol), potassium thyocianate (0.523 g, 5.39 mmol), and 3-(aminomethyl)-pyridine (0.540 mL, 5.39 mmol). The crude product was purified with several methanol washes to afford a white solid (1.125 mg, 58%); mp 153−154 °C. ^{1}H NMR ($CDCl_3$) δ 12.74 (s, 1H), 8.74 (s, 1H), 8.59 (d, J = 4.8 Hz, 1H), 8.38 (bs, 1H), 8.00 (d, J = 7.5 Hz, 1H), 7.94−7.76 (m, 1H), 7.55 (d, J = 8.0 Hz, 1H), 7.43 − 6.96 (m, 9H), 6.50 (d, J = 7.5 Hz, 2H), 5.09 (d, J = 4.8 Hz, 2H). ^{13}C NMR ($CDCl_3$) δ 181.8, 156.6, 149.6, 143.2, 132.3, 131.5, 129.3, 127.9, 124.8, 122.9, 117.9, 47.3. HPLC: purity 97%, rt = 3.94 min. MS (ESI+): 397 [M + H].

1-(2-Hydroxyethyl)-3-(*N*-1-naphthylbenzimidoyl)thiourea (20). *N*-Naphthyl-benzimidoyl chloride (1.940 g, 4.9 mmol), potassium thyocianate (0.523 g, 5.39 mmol), and 2-aminoethanol (0.325 mL, 5.39 mmol). The crude product was purified with several methanol washes to afford a white solid (410 mg, 24%); mp 131−132 °C. ^{1}H NMR ($CDCl_3$) δ 12.43 (s, 1H), 8.25 (s, 1H), 8.14 (d, J = 7.2 Hz, 1H), 7.82 (d, J = 6.5 Hz, 1H), 7.65−7.40 (m, 1H), 7.40−6.86 (m, 7H), 6.45 (d, J = 6.8 Hz, 2H), 3.94 (s, 4H,), 2.16 (s, 1H). ^{13}C NMR ($CDCl_3$) δ 181.3, 155.9, 143.1, 133.9, 132.0, 130.6, 128.7, 128.1, 128.1, 127.5, 126.3, 126.1, 125.5, 124.0, 123.2, 117.2, 61.5, 47.7. HPLC: purity 96%, rt = 4.82 min. MS (ESI+): 350 [M + H].

3-(*N*-Phenyl-1-naphthylacetimidoyl)-1-(3-pyridylmethyl)-thiourea (21). *N*-Phenyl-1-naphthylacetimidoyl chloride (2.178 g, 5.5 mmol), potassium thyocianate (0.588 g, 6.06 mmol), and 3-(aminomethyl)pyridine (0.613 mL, 6.06 mmol). The crude product was purified with several methanol washes to afford a white solid (1.285 mg, 59%); mp 162−163 °C. ^{1}H NMR ($CDCl_3$) δ 12.65 (s, 1H), 8.76 (s, 1H), 8.60 (d, J = 3.6 Hz, 1H), 8.14 (bs, 1H), 8.00 (d, J = 8.1 Hz, 1H), 7.95−7.64 (m, 3H), 7.70−7.11 (m, 6H), 7.06−6.40 (m, 4H), 5.07 (s, 2H). ^{13}C NMR ($CDCl_3$) δ 181.1, 155.8, 149.3, 149.0, 145.9, 135.9, 133.2, 132.9, 130.7, 130.0, 128.5, 128.4, 127.6, 127.3, 126.9, 126.7, 125.2, 124.8, 124.5, 124.2, 123.6, 121.7, 120.0, 46.8. HPLC: purity 98%, rt = 3.90 min. MS (ESI+): 397 [M + H].

1-(2-Hydroxyethyl)-3-(*N*-phenyl-1-naphthylacetimidoyl)-thiourea (22). *N*-Phenyl-1-naphthylacetimidoyl chloride (2.158 g, 5.45 mmol), potassium thyocianate (0.583 g, 6.00 mmol), and 2-aminoethanol (0.362 mL, 6.00 mmol). The crude product was purified with several methanol washes to afford a white solid (932 mg, 49%); mp 155−156 °C. ^{1}H NMR ($CDCl_3$) δ 12.34 (s, 1H), 8.25 (s, 1H), 8.02−7.63 (m, 2H), 7.8−7.24 (m, 2H), 7.27−6.44 (m, 8H), 3.95 (s, 4H), 2.32 (s, 1H). ^{13}C NMR ($CDCl_3$) δ 181.0, 133.1, 130.6, 130.0,

128.5, 127.5, 126.9, 124.7, 124.1, 121.8, 61.3, 47.6. HPLC: purity 96%, rt = 4.71 min. MS (ESI+): 350 [M + H].

3-(*N*-Phenylacetimidoyl)-1-(3-pyridylmethyl)thiourea (23). *N*-Phenyl-acetimidoyl chloride (0.330 g, 2.16 mmol), potassium thyocianate (0.231 g, 2.38 mmol), and 3-(aminomethyl)pyridine (0.240 mL, 2.38 mmol). The crude product was purified by flash chromatography (AcOEt/hexane 1:1) to afford a white solid (196 mg, 32%); mp 143−144 °C. ^{1}H NMR ($CDCl_3$) δ 12.39 (s, 1H), 8.71 (s, 1H), 8.61 (s, 1H) 8.56 (d, J = 4.3 Hz, 1H), 7.79−7.55 (m, 1H), 7.36−7.14 (m, 2H), 7.05 (m, 2H), 6.85−6.46 (m, 2H), 5.10−4.64 (m, 2H), 1.88 (s, 3H). ^{13}C NMR ($CDCl_3$) δ 181.1, 155.6, 149.0, 148.8, 146.6, 135.4, 132.8, 128.9, 124.2, 123.5, 121.2, 119.8, 46.4, 18.1. HPLC: purity 95%, rt = 2.96 min. MS (ESI+): 285 [M + H].

3-(*N*-Phenylhexanoimidoyl)-1-(3-pyridylmethyl)thiourea (24). *N*-Phenylhexanoimidoyl chloride (1.360 g, 6.50 mmol), potassium thyocianate (0.761 g, 7.84 mmol), and 3-(aminomethyl)-pyridine (0.793 mL, 7.84 mmol). The crude product was purified by flash chromatography (AcOEt/hexane 1:2) to afford a yellow solid (332 mg, 15%); mp 94−95 °C. ^{1}H NMR ($CDCl_3$) δ 12.45 (s, 1H), 8.61 (d, J = 0.8 Hz, 1H), 8.52 (t, J = 5.6 Hz, 1H), 8.38 (m, 1H), 7.72 (t, J = 8.0 Hz, 1H), 7.40−7.18 (m, 3H), 7.09 (t, J = 7.3 Hz, 1H), 6.74 (d, J = 7.6 Hz, 2H), 4.93 (d, J = 5.4 Hz, 2H), 2.21 (t, J = 7.9 Hz, 2H), 1.54 (s, 2H), 1.17 (m, 2H), 0.80 (t, J = 6.5 Hz, 3H). ^{13}C NMR ($CDCl_3$) δ 181.0, 174.2, 149.6, 149.4, 135.7, 132.3, 129.4, 129.1, 125.7, 123.7, 120.2, 46.9, 37.4, 31.3, 24.5, 22.4, 13.9. HPLC: purity 95%, rt = 4.22 min. MS (ESI+): 341 [M + H].

1-(4-Morpholinethyl)-3-(*N*-phenylbenzimidoyl)thiourea (25). *N*-Phenyl-benzimidoyl chloride (1.900 g, 8.84 mmol), potassium thyocianate (1.267 g, 9.73 mmol), and 2-(4-morpholinyl) ethanamine (1.267 mL, 9.73 mmol). The crude product was purified with several methanol washes to afford a pale-yellow solid (2.28 g, 70%); mp 167−168 °C. ^{1}H NMR ($CDCl_3$) δ 12.09 (s, 1H), 7.97 (s, 1H), 7.30−6.88 (m, 8H), 6.62 (d, 2H, J = 7.5 Hz), 3.75 (m, 2H), 3.41 (m, 4H), 2.56 (m, 2H), 2.42 (m, 4H). ^{13}C NMR ($CDCl_3$) δ 179.7, 154.9, 132.0, 130.7, 130.4, 129.0, 128.9, 128.7, 128.0, 124.0, 122.4, 66.7, 55.9, 53.1, 42.7. HPLC: purity >99%, rt = 2.85 min. MS (ESI+): 370 [M + H].

3-(*N*-Benzylbenzimidoyl)-1-(3-pyridylmethyl)thiourea (26). *N*-Benzyl-benzimidoyl chloride (0.54 g, 2.36 mmol), potassium thyocianate (0.25 g, 2.59 mmol), and 3-(aminomethyl)pyridine (0.26 mL, 2.59 mmol). The crude product was purified by recrystallization from MeOH/H_2O to afford a pale-yellow solid (263 mg, 31%); mp 104−105 °C. ^{1}H NMR ($CDCl_3$) δ 12.96 (s, 1H), 8.56 (m, 2H), 7.99 (s, 2H), 7.86−6.84 (m, 10H), 4.88 (s, 2H), 4.38 (s, 2H). ^{13}C NMR ($CDCl_3$) δ 181.0, 157.6, 149.4, 149.0, 139.5, 135.7, 132.6, 130.7, 129.2, 128.6, 128.5, 128.4, 127.0, 126.7, 123.5, 54.3, 46.8. HPLC: purity 95%, rt = 3.03 min. MS (ESI+): 361 [M + H].

3-(*N*-Phenylbenzimidoyl)-1-(2-pyridyl)thiourea (27). *N*-Phenyl-benzimidoyl chloride (5.44 g, 25.3 mmol), potassium thyocianate (2.71 g, 27.9 mmol), and 2-aminopyridine (2.62 g, 27.9 mmol). The crude product was purified by several methanol washes to afford a yellow solid (8.40 g, 84%); mp 123−124 °C. ^{1}H NMR ($CDCl_3$) δ 14.44 (s, 1H), 8.83 (d, J = 8.3 Hz, 1H), 8.39 (s, 1H), 8.05 (d, J = 5.1 Hz, 1H), 7.75 (d, J = 7.2 Hz, 1H), 7.32 (d, J = 7.2 Hz, 3H), 7.10 (m, 4H), 6.79 (d, J = 7.2 Hz, 2H), 6.70−6.43 (m, 2H). ^{13}C NMR (DMSO) δ 183.4, 160.4, 153.2, 148.3, 137.6, 131.3, 129.3, 128.9, 128.3, 124.8, 121.7, 112.6, 108.7, 107.2. HPLC: purity 97%, rt = 4.77 min. MS (ESI+): 333 [M + H].

General Procedure for Hydrobromide Iminothiadiazole Synthesis. Over a mixture of the corresponding imidoylthiourea (1 equiv) in CH_2Cl_2 /AcOEt (1:2) at 0 °C, a solution of Br_2 in AcOEt (0.5 M, 2 equiv) was added dropwise. Upon completion of the addition, the resulting mixture was left stirring at 4 °C until starting material clearance (1−12 h). Then the precipitate formed was isolated, washed with a mixture of pentane:ethyl acetate (3:1), and purified by recrystallization from MeOH/H_2O.

2,3-Diphenyl-5-(3-pyridinylmethylimino)-2,5-dihydro-1,2,4-thiadiazole Dihydrobromide (28). Imidoylthiourea **1** (0.608 g, 1.75 mmol) and bromine (0.180 mL, 3.5 mmmol). Reaction time: 1 h. White solid (566 mg, 64%); mp 255−256 °C. ^{1}H NMR (DMSO) δ 10.39 (t, J = 6.0 Hz; 1H), 8.99 (s, 1H), 8.83 (d, J = 4.5 Hz; 1H), 8.51 (d, J = 8.0 Hz; 1H), 7.98 (dd, J = 7.9, 5.6 Hz, 1H), 7.62−7.26 (m, 10H), 5.13 (d, J = 5.9 Hz; 2H). ^{13}C NMR (DMSO) δ 176.7, 165.3, 144.1, 143.7, 136.6, 135.0, 133.4, 131.6, 130.9, 129.4, 128.2, 127.2, 127.1, 45.6. ^{15}N NMR (DMSO) δ 250, 197, 145, 131. MS (ESI+): 345 [M − HBr_2]. Anal. ($C_{20}H_{18}Br_2N_4S$) C, H, Br, N, S.

5-Ethoxycarbonylmethylimino-2,3-diphenyl-2,5-dihydro-1,2,4-thiadiazole Hydrobromide (29). Imidoylthiourea **2** (0.219 g, 0.64 mmol) and bromine (0.065 mL, 1.26 mmol). Reaction time: 1 h. White solid (172 mg, 64%); mp 232−233 °C. ^{1}H NMR (DMSO) δ 10.05 (s, 1H), 7.68−7.29 (m, 10H), 4.60 (s, 2H), 4.19 (q, J = 7.1 Hz; 2H), 1.22 (t, J = 7.1 Hz; 3H). ^{13}C NMR (DMSO) δ 176.8, 169.3, 165.3, 135.0, 134.4, 133.4, 131.8, 131.5, 131.2, 130.9, 130.9, 129.8, 129.4, 128.3, 127.1, 61.9, 46.6, 14.8. ^{15}N NMR (DMSO) δ 260, 200, 130. MS (ESI+): 340 [M − Br]. Anal. ($C_{18}H_{18}BrN_3O_2S$) C, H, Br, N, S.

5-(2-Hydroxyethylimino)-2,3-diphenyl-2,5-dihydro-1,2,4-thiadiazole Hydrobromide (30). Imidoylthiourea **3** (0.500 g, 1.65 mmol) and bromine (0.167 mL, 3.25 mmol). Reaction time: 4 h. White solid (187 mg, 30%); mp 235−236 °C. ^{1}H NMR (DMSO) δ 10.00 (bs, 1H), 7.72−7.29 (m, 10H), 4.31 (bs, 1H), 3.80 (q, J = 6.1 Hz; 2H), 3.69 (t, J = 5.2 Hz; 2H). ^{13}C NMR (DMSO) δ 175.7, 165.3, 134.4, 132.6, 130.8, 130.2, 128.6, 127.6, 126.6, 58.8, 47.4. MS (ESI+): 298 [M − Br]. Anal. ($C_{16}H_{16}BrN_3OS$) C, H, Br, N, S.

5-Imino-2,3-diphenyl-2,5-dihydro-1,2,4-thiadiazole Hydrobromide (31). Imidoylthiourea **4** (0.20 g, 0.78 mmol) and bromine (0.081 mL, 1.54 mmol). Reaction time: 12 h. White solid (78 mg, 30%); mp 248−249 °C. ^{1}H NMR (DMSO) δ 10.48 (s, 1H), 9.45 (s, 1H), 7.83−7.00 (m, 10H). ^{13}C NMR (DMSO) δ 178.9, 166.0, 134.9, 132.8, 131.0, 130.5, 130.5, 129.0, 128.0, 126.9. MS (ESI+): 254 [M − Br]. Anal. ($C_{14}H_{12}BrN_3S$) C, H, Br, N, S.

5-Pentylimino-2,3-diphenyl-2,5-dihydro-1,2,4-thiadiazole Hydrobromide (32). Imidoylthiourea **5** (0.20 g, 0.62 mmol) and bromine (0.063 mL, 1.22 mmol). Reaction time: 12 h. In this case, no precipitate was formed. Solvent was evaporated under reduced pressure, and the crude was washed with a mixture pentane:ethyl acetate (3:1). The crude was purified by MeOH/H_2O recrystallization to afford a pale-brown solid (104 mg, 42%); mp 241−242 °C. ^{1}H NMR (DMSO) δ 10.05 (s, 1H), 7.75−7.19 (m, 10H), 3.73 (m; 2H), 1.78−1.61 (m, 2H), 1.51−1.22 (m, 4H), 0.91 (t, J = 7.0 Hz; 3H). ^{13}C NMR (DMSO) δ 175.6, 165.6, 134.8, 132.9, 131.1, 130.6, 130.6, 129.0, 128.0, 127.0, 45.2, 28.7, 28.4, 22.0, 14.2. MS (ESI+): 324 [M − Br]. Anal. ($C_{19}H_{22}BrN_3S$) C, H, Br, N, S.

2,3-Diphenyl-5-phenylimino-2,5-dihydro-1,2,4-thiadiazole Hydrobromide (33). Imidoylthiourea **6** (0.20 g, 0.60 mmol) and bromine (0.061 mL, 1.19 mmol). Reaction time: 12 h. Yellow solid (132 mg, 54%); mp 230−231 °C. (lit.[21] 227−228 °C). ^{1}H NMR (DMSO) δ 12.41 (s, 1H), 8.50−6.51 (m, 15H). ^{13}C NMR (DMSO) δ 178.6, 171.1, 142.8, 139.7, 138.5, 136.7, 136.1, 135.9, 135.4, 134.4, 133.3, 132.1, 131.6, 125.7, 100.0. MS (ESI+): 330 [M − Br]. Anal. ($C_{20}H_{16}BrN_3S$) C, H, Br, N, S.

5-Cyclohexylimino-2,3-diphenyl-2,5-dihydro-1,2,4-thiadiazole Hydrobromide (34). Imidoylthiourea **7** (0.854 g, 2.53 mmol) and bromine (0.26 mL, 5.07 mmol). Reaction time: 12 h. Pale-brown solid (273 mg, 26%); mp 236−237 °C (lit.[43] 235−237 °C). ^{1}H NMR (DMSO) δ 10.19 (bs, 1H), 7.98−6.96 (m, 10H), 4.20 (m, 1H), 1.95 (m, 2H), 1.72 (m, 2H), 1.62−1.24 (m, 6H). ^{13}C NMR (DMSO) δ 174.9, 166.2, 134.8, 132.9, 131.2, 130.6, 129.0, 128.0, 127.0, 54.1, 31.6, 25.2, 23.7. MS (ESI+): 336 [M − Br]. Anal. ($C_{20}H_{22}BrN_3S$) C, H, Br, N, S.

2-(4-Methoxyphenyl)-3-phenyl-5-(3-pyridinylmethylimino)-2,5-dihydro-1,2,4-thiadiazole Dihydrobromide (35). Imidoylthiourea **8** (0.400 g, 1.06 mmol) and bromine (0.109 mL, 2.12 mmol). Reaction time: 3 h. White solid (62 mg, 13%); mp 192−193 °C. ^{1}H NMR (DMSO) δ 10.42 (t, J = 5.9 Hz, 1H), 9.08 (s, 1H), 8.92 (d, J = 5.3 Hz, 1H), 8.68 (d, J = 8.2, 1H), 8.13 (dd, J = 7.9 Hz, 5.8 Hz, 1H), 7.76−7.24 (m, 7H), 7.06 (d, J = 8.9 Hz, 2H), 5.17 (d, J = 5.9 Hz, 2H), 3.79 (s, 3H). ^{13}C NMR (DMSO) δ 176.6, 165.4, 161.3, 144.6, 143.1, 136.4, 133.3, 130.9, 129.7, 129.4, 127.3, 127.2, 126.8, 116.0, 56.4, 45.5. MS (ESI+): 375 [M − HBr_2]. Anal. ($C_{21}H_{20}Br_2N_4OS$) C, H, Br, N, S.

5-Ethoxycarbonylmethylimino-2-(4-methoxyphenyl)-3-phenyl-2,5-dihydro-1,2,4-thiadiazole Hydrobromide (36). Imidoylthiourea **9** (0.400 g, 1.07 mmol) and bromine (0.110 mL, 2.15 mmol). Reaction time: 2 h. White solid (48 mg, 10%); mp 189−190 °C. ^{1}H NMR (DMSO) δ 9.90 (t, J = 5.5 Hz, 1H), 7.79−7.24 (m, 7H), 7.06 (d, J = 8.9 Hz, 2H), 4.58 (d, J = 5.7 Hz, 2H), 4.20 (q, J = 7.1 Hz, 2H), 3.79 (s, 3H), 1.23 (t, J = 7, 1 Hz, 3H). ^{13}C NMR (DMSO): δ 176.0, 168.1, 165.0, 160.6, 132.6, 130.2, 129.1, 128.6, 126.5, 115.2, 61.2, 55.6, 45.8, 14.0. MS (ESI+): 370 [M − Br]. Anal. ($C_{19}H_{20}BrN_3O_3S$) C, H, Br, N, S.

2-(4-Nitrophenyl)-3-phenyl-5-(3-pyridinylmethylimino)-2,5-dihydro-1,2,4-thiadiazole Dihydrobromide (37). Imidoylthiourea **10** (0.700 g, 1.79 mmol) and bromine (0.184 mL, 3.58 mmol). Reaction time: 3 h. Yellow solid (128 mg, 13%); mp 242−243 °C. ^{1}H NMR (DMSO) δ 10.51 (s, 1H), 9.03 (s, 1H), 8.87 (d, J = 5.4 Hz, 1H), 8.56 (d, J = 8.0 Hz, 1H), 8.38 (d, J = 9.0 Hz, 2H), 8.02 (dd, J = 8.0 Hz, 5.5, 1H), 7.83 (d, J = 9.0 Hz, 2H), 7.64−7.38 (m, 5H), 5.19 (d, J = 5.0 Hz, 2H). ^{13}C NMR (DMSO) δ 176.7, 165.2, 148.4, 143.7, 140.2, 136.3, 133.8, 130.8, 129.4, 129.2, 126.8, 126.6, 125.8, 45.4. MS (ESI+): 390 [M − HBr_2]. Anal. ($C_{20}H_{17}Br_2N_5O_2S$) C, H, Br, N, S.

5-Ethoxycarbonylmethylimino-2-(4-nitrophenyl)-3-phenyl-2,5-dihydro-1,2,4-thiadiazole Hydrobromide (38). Imidoylthiourea **11** (0.600 g, 1.55 mmol) and bromine (0.160 mL, 3.1 mmol). Reaction time: 4 h. Pale-yellow solid (461 mg, 64%); mp 225−226 °C. ^{1}H NMR (DMSO) δ 10.00 (t, J = 5.7 Hz, 1H), 8.37 (d, J = 8.9 Hz, 2H), 7.87 (d, J = 8.9 Hz, 2H), 7.67−7.20 (m, 5H), 4.62 (d, J = 5.6 Hz, 2H), 4.20 (q, J = 7.1 Hz, 2H), 1.23 (t, J = 7.1 Hz, 3H). ^{13}C NMR (DMSO) δ 176.8, 168.3, 165.5, 148.4, 140.1, 133.3, 130.8, 129.5, 129.2, 126.6, 125.8, 61.6, 46.4, 14.4. MS (ESI+): 385 [M − Br]. Anal. ($C_{18}H_{17}BrN_4O_4S$) C, H, Br, N, S.

5-(2-Hydroxyethylimino)-2-(4-methoxyphenyl)-3-phenyl-2,5-dihydro-1,2,4-thiadiazole Hydrobromide (39). Imidoylthiourea **12** (0.400 g, 1.22 mmol) and bromine (0.120 mL, 2.44 mmol). Reaction time: 2 h. White solid (49 mg, 10%); mp 195−196 °C. ^{1}H NMR (DMSO) δ 9.89 (t, J = 5.3, 1H), 7.58−7.49 (m, 5H), 7.43 (d, J = 9.7 Hz, 2H), 7.05 (d, J = 8.9, 2H), 3.78 (s, 3H), 3.76 (m, 2H), 3.68 (m, 2H), 3.33 (bs, 1H). ^{13}C NMR (DMSO) δ 175.9, 165.7, 160.9, 132.9, 130.6, 129.5, 129.0, 127.1, 127.0, 115.6, 59.2, 56.0, 47.7. MS (ESI+): 329 [M − Br]. Anal. ($C_{19}H_{20}BrN_3O_3S$) C, H, Br, N, S.

3-(4-Methoxyphenyl)-2-phenyl-5-(3-pyridylmethylimino)-2,5-dihydro-1,2,4-thiadiazole Dihydrobromide (40). Imidoylthiourea **13** (0.606 g, 1.6 mmol) and bromine (0.166 mL, 3.22 mmol). Reaction time: 3 h. White solid (483 mg, 56%); mp 204−205 °C. ^{1}H NMR (DMSO) δ 10.39 (s, 1H), 9.06 (d, J = 1.7 Hz, 1H), 8.98−8.82 (m, 1H), 8.62 (dt, J = 8.1 Hz, 1.5 Hz, 1H), 8.07 (dd, J = 7.9 Hz, 5.8 Hz, 1H), 7.68−7.37 (m, 7H), 7.09−6.80 (m, 2H), 5.17 (d, J = 5.8 Hz, 2H), 3.77 (s, 3H). ^{13}C NMR (DMSO) δ 175.4, 163.9, 162.7, 143.8, 142.7, 136.3, 134.7, 132.6, 130.8, 130.4, 127.5, 126.6, 118.3, 114.2, 55.6, 44.7. MS (ESI+): 375 [M − HBr_2]. Anal. ($C_{21}H_{20}Br_2N_4OS$) C, H, Br, N, S.

5-(2-Hydroxyethylimino)-3-(4-methoxyphenyl)-2-phenyl-2,5-dihydro-1,2,4-thiadiazole Hydrobromide (41). Imidoylthiourea **14** (0.600 g, 1.82 mmol) and bromine (0.187 mL, 3.65 mmol). Reaction time: 4 h. White solid (341 mg, 46%); mp 193−194 °C. ^{1}H NMR (DMSO) δ 9.94 (t, J = 4.9 Hz, 1H), 7.82−7.18 (m, 7H), 6.96 (d, J = 9.0 Hz, 2H), 3.92−3.53 (m, 7H), 3.34 (bs, 1H). ^{13}C NMR (DMSO) δ 175.0, 164.6, 162.6, 134.8, 132.5, 130.7, 130.3, 127.6, 118.4, 114.2, 58.8, 55.6, 47.3. MS (ESI+): 329 [M − Br]. Anal. ($C_{17}H_{18}BrN_3O_2S$) C, H, Br, N, S.

5-Ethoxycarbonylmethylimino-3-(4-methoxyphenyl)-2-phenyl-2,5-dihydro-1,2,4-thiadiazole Hydrobromide (42). Imidoylthiourea **15** (0.400 g, 1.08 mmol) and bromine (0.110 mL, 2.16 mmol). Reaction time: 2 h. White solid (150 mg, 31%); mp 171−172 °C. ^{1}H NMR (DMSO) δ 9.89 (t, J = 5.6 Hz, 1H), 7.71−7.56 (m, 5H), 7.45 (d, J = 9.0 Hz, 2H), 6.96 (d, J = 9.0 Hz, 2H), 4.58 (s, 2H), 4.20 (q, J = 7.1 Hz, 2H), 3.77 (s, 3H), 1.24 (t, J = 7.1 Hz, 3H). ^{13}C NMR (DMSO) δ 173.25, 168.8, 164.9, 163.4, 135.3, 133.3, 131.6, 131.1, 128.3, 119.0, 115.0, 61.9, 56.4, 46.5, 14.8. MS (ESI+): 370 [M − Br]. Anal. ($C_{19}H_{20}BrN_3O_3S$) C, H, Br, N, S.

3-(4-Methoxyphenyl)-5-pentylimino-2-phenyl-2,5-dihydro-1,2,4-thiadiazole Hydrobromide (43). Imidoylthiourea **16** (0.637 g, 1.79 mmol) and bromine (0.184 mL, 3.59 mmol). Reaction time: 12 h. Pale-brown solid (327 mg, 42%); mp 176−177 °C. ^{1}H NMR (DMSO) δ 10.01 (s, 1H), 7.72−7.45 (m, 7H), 6.95 (d, J = 9.0 Hz, 2H), 3.76 (s, 3H), 3.71 (m, 2H), 1.67 (m, 2H), 1.49−1.27 (m, 4H), 0.89 (t, J = 7.1 Hz, 3H). ^{13}C NMR (DMSO) δ 174.5, 164.5, 162.6, 134.9, 132.5, 130.7, 130.3, 127.6, 118.5, 114.2, 55.6, 44.6, 28.3, 28.0, 21.6, 13.8. ^{15}N NMR (DMSO) δ 245, 206, 133. MS (ESI+): 354 [M − Br]. Anal. ($C_{20}H_{25}BrN_3OS$) C, H, Br, N, S.

3-(4-Methoxyphenyl)-2-phenyl-5-phenylimino-2,5-dihydro-1,2,4-thiadiazole Hydrobromide (44). Imidoylthiourea **17** (0.600 g, 1.81 mmol) and bromine (0.186 mL, 3.62 mmol). Reaction time: 12 h. Pale-yellow solid (120 mg, 15%); mp 217−218 °C (lit.[44] 218 °C). ^{1}H NMR (DMSO) δ 12.23 (s, 1H), 8.01−6.73 (m, 14H), 3.79 (s, 3H). ^{13}C NMR (DMSO) δ 178.7, 166.9, 160.2, 139.9, 131.1, 130.2, 129.5, 128.3, 123.3, 118.9, 113.4, 55.6. MS (ESI+): 360 [M − Br]. Anal. ($C_{21}H_{18}BrN_3OS$) C, H, Br, N, S.

3-(4-Trifluoromethylphenyl)-2-phenyl-5-(3-pyridylmethylimino)-2,5-dihydro-1,2,4-thiadiazole Dihydrobromide (45). Imidoylthiourea **18** (0.300 g, 0.72 mmol) and bromine (0.074 mL, 1.45 mmol). Reaction time: 4 h. White solid (60 mg, 33%); mp 177−178 °C. ^{1}H NMR (DMSO) δ 10.84 (t, J = 6.0 Hz, 1H), 9.01 (s, 1H), 8.88 (d, J = 5.3 Hz, 1H), 8.59 (d, J = 8.0 Hz, 1H), 8.05 (dd, J = 7.9, 5.6 Hz, 1H), 7.82 (d, J = 8.5 Hz, 2H), 7.80−7.62 (m, 2H), 7.64−7.41 (m, 5H), 5.15 (d, J = 6.0 Hz, 2H). ^{13}C NMR (DMSO) δ 176.7, 162.9, 145.5, 141.4, 137.0, 133.9, 131.1, 130.9, 130.2, 127.4, 125.6, 125.5, 44.6. MS (ESI+): 413 [M − HBr_2]. Anal. ($C_{21}H_{17}F_3Br_2N_4S$) C, H, Br, N, S.

2-(1-Naphthyl)-3-phenyl-5-(3-pyridylmethylimino)-2,5-dihydro-1,2,4-thiadiazole Dihydrobromide (46). Imidoylthiourea **19** (0.600 g, 1.51 mmol) and bromine (0.156 mL, 3.03 mmol). Reaction time: 24 h. White solid (674 mg, 80%); mp 205−206 °C. ^{1}H NMR (DMSO) δ 10.52 (s, 1H), 9.09 (s, 1H), 8.90 (d, J = 5.2 Hz, 1H), 8.65 (d, J = 8.0 Hz, 1H), 8.28−7.24 (m, 13H), 5.24 (d, J = 5.2 Hz, 2H). ^{13}C NMR (DMSO) δ 176.7, 165.4, 143.8, 142.9, 142.8, 136.2, 133.7, 132.9, 131.7, 130.3, 129.6, 128.9, 128.8, 128.7, 127.8, 127.6, 126.6, 126.5, 125.8, 121.7, 45.0. MS (ESI+): 395 [M − HBr_2]. Anal. ($C_{24}H_{20}Br_2N_4S$) C, H, Br, N, S.

5-(2-Hydroxyethylimino)-2-(1-naphthyl)-3-phenyl-2,5-dihydro-1,2,4-thiadiazole Hydrobromide (47). Imidoylthiourea **20** (0.418 g, 1.97 mmol) and bromine (0.123 mL, 2.39 mmol). Reaction time: 24 h. White solid (266 mg, 52%) mp 154−155 °C. ^{1}H NMR (DMSO) δ 10.19 (t, J = 5.7 Hz, 0.5H, *E*-NH), 10.10 (t, J = 5.6 Hz, 0.5H, *Z*-NH), 8.24−8.14 (m, 1H), 8.16 8.06 (m, 2H), 8.00−7.92 (m, 1H), 7.92−7.83 (m, 2H), 7.71−7.52 (m, 2H), 7.56−7.38 (m, 2H), 7.38−7.13 (m, 2H), 4.36 (t, J = 5.3 Hz, 1H, *E*-CH_2-N), 4.07 (dd, J = 7.6, 5.8 Hz, 1H, *E*-CH_2), 3.87 (dd, J = 8.2, 5.2 Hz, 1H, *Z*-CH_2), 3.74 (t, J = 5.8 Hz, 1H, *Z*-CH_2-N). ^{13}C NMR (DMSO) δ 176.9, 166.8, 134.2, 133.3, 132.1, 130.8, 130.0, 129.4, 129.2, 129.1, 128.4, 127.0, 127.0, 122.1, 62.3 (*E*-CH_2-N), 59.3 (*Z*-CH_2-N), 48.1 (*Z*-CH_2), 44.5 (*E*-CH_2). MS (ESI+): 348 [M − Br]. Anal. ($C_{20}H_{18}BrN_3OS$) C, H, Br, N, S.

3-(1-Naphthyl)-2-phenyl-5-(3-pyridylmethylimino)-2,5-dihydro-1,2,4-thiadiazole Dihydrobromide (48). Imidoylthiourea **21** (0.600 g, 1.52 mmol) and bromine (0.155 mL, 3.03 mmol). Reaction time: 24 h. Gray solid (540 mg, 64%); mp 177−178 °C. ^{1}H NMR (DMSO) δ 10.56 (s, 1H), 8.87 (m 1H), 8.83 (d, J = 5.0 Hz, 1H), 8.41 (d, J = 7.8 Hz, 1H), 8.06 (d, J = 8.1 Hz, 1H), 7.95 (m, 4H), 7.69−7.25 (m, 8H), 5.08 (d, J = 5.0 Hz, 2H). ^{13}C NMR (DMSO) δ 176.9, 165.4, 145.1, 144.1, 142.1, 141.7, 138.9, 135.4, 133.9, 132.7, 130.4, 129.8, 128.4, 127.6, 126.9, 125.1, 124.3, 123.9, 121.6, 45.1. MS (ESI+): 395 [M − HBr_2]. Anal. ($C_{24}H_{20}Br_2N_4S$) C, H, Br, N, S.

5-(2-Hydroxyethylimino)-3-(1-naphthyl)-2-phenyl-2,5-dihydro-1,2,4-thiadiazole Hydrobromide (49). Imidoylthiourea **22** (0.600 g, 1.72 mmol) and bromine (0.176 mL, 3.44 mmol). Reaction time: 24 h. White solid (147 mg, 20%); mp 163−164 °C. ^{1}H NMR (DMSO) δ 10.21 (t, J = 5.3 Hz, 1H), 8.08 (m, 2H), 7.97 (m, 2H), 7.78−7.65 (m, 1H), 7.68−7.15 (m, 7H), 3.74 (m, 2H), 3.65 (t, J = 4.9 Hz, 2H), 3.49 (s, 1H). ^{13}C NMR (DMSO) δ 177.0, 166.5, 134.6, 133.4, 132.7, 131.0, 130.5, 130.4, 130.2, 129.1, 128.4, 127.8, 127.6,

dx.doi.org/10.1021/jm201463v | J. Med. Chem. 2012, 55, 1645−1661

125.7, 125.5, 124.8, 59.5, 48.2. MS (ESI+): 348 [M − Br]. Anal. ($C_{20}H_{18}BrN_3OS$) C, H, Br, N, S.

3-Methyl-2-phenyl-5-(3-pyridylmethylimino)-2,5-dihydro-1,2,4-thiadiazole Dihydrobromide (50). Imidoylthiourea **23** (1.00 g, 3.52 mmol), bromine (0.362 mL, 7.04 mmol). Reaction time: 2 h. White solid (390 mg, 25%); mp 109−110 °C. ^{1}H NMR (DMSO) δ 10.36 (s, 1H), 9.00 (s, 1H), 8.89 (d, J = 5.0 Hz, 1H), 8.58 (d, J = 8.0 Hz, 1H), 8.03 (m, 1H), 7.58 (m, 5H), 5.09 (d, J = 5.6 Hz, 2H), 2.35 (s, 3H). ^{13}C NMR (DMSO) δ 176.3, 168.2, 143.2, 143.0, 135.9, 133.5, 133.2, 131.0, 130.2, 127.2, 126.4, 44.7, 16.3. MS (ESI+): 283 [M − HBr_2]. Anal. ($C_{15}H_{16}Br_2N_4S$) C, H, Br, N, S.

3-Pentyl-2-phenyl-5-(3-pyridylmethylimino)-2,5-dihydro-1,2,4-thiadiazole Dihydrobromide (51). Imidoylthiourea **24** (0.30 g, 0.88 mmol) and bromine (0.090 mL, 1.76 mmol). Reaction time: 24 h. Yellow solid (57 mg, 13%); mp 143−144 °C. ^{1}H NMR (DMSO) δ 10.26 (t, J = 5.8 Hz, 1H), 8.98 (s, 1H), 8.87 (d, J = 4.9 Hz, 1H), 8.53 (d, J = 8.1 Hz, 1H), 8.02 (dd, J = 7.9, 5.7 Hz, 1H), 7.64 (m, 5H), 5.06 (d, J = 5.7 Hz, 2H), 2.54 (t, J = 7.5 Hz, 2H), 1.92−1.32 (m, 2H), 1.18−1.11 (m, 4H), 0.76 (t, J = 6.9 Hz, 3H). ^{13}C NMR (DMSO) δ 176.5, 170.9, 143.4, 143.0, 136.1, 132.9, 131.1, 130.2, 129.8, 127.4, 126.4, 123.1, 44.8, 30.2, 28.7, 25.6, 21.5, 13.6. MS (ESI+): 339 [M − HBr_2]. Anal. ($C_{19}H_{24}Br_2N_4S$) C, H, Br, N, S.

5-(4-Morpholinethylimino)-2,3-diphenyl-2,5-dihydro-1,2,4-thiadiazole Dihydrobromide (55). Imidoylthiourea **25** (0.60 g, 1.63 mmol) and bromine (0.160 mL, 3.26 mmol). Reaction time: 3 h. White solid (438 mg, 51%); mp 241−242 °C. ^{1}H NMR (DMSO) δ 10.11 (s), 7.52−7.4 (m, 10H), 4.18(m, 2H), 4.01 (m, 2H), 3.78−3.45 (m, 8H). ^{13}C NMR (DMSO) δ 176.3, 164.4, 134.2, 133.1, 131.2, 130.8, 130.8, 129.3, 128.2, 126.25, 63.2, 54.3, 52.0, 38.9. ^{15}N NMR (DMSO) δ 252, 212, 130, 16. MS (ESI+): 367 [M − HBr_2]. Anal. ($C_{20}H_{24}Br_2N_4OS$) C, H, Br, N, S.

2-Benzyl-3-phenyl-5-(3-pyridylmethylimino)-2,5-dihydro-1,2,4-thiadiazole Dihydrobromide (58). Imidoylthiourea **26** (0.224 g, 0.62 mmol), bromine (0.063 mL, 1.24 mmol). Reaction time: 12 h. White solid (26 mg, 8%); mp 139−140 °C. ^{1}H NMR (DMSO) δ 10.22 (t, J = 5.8 Hz, 1H), 8.85 (s, 1H), 8.75 (d, J = 5.3 Hz, 1H), 8.32 (d, J = 8.0 Hz, 1H), 7.88−7.74 (m, 3H), 7.71−7.55 (m, 3H), 7.43−7.27 (m, 5H), 5.40 (s, 2H), 4.99 (d, J = 5.7 Hz, 2H). ^{13}C NMR (DMSO) δ 176.4, 167.6, 144.2, 143.5, 136.8, 135.2, 133.4, 130.3, 129.8, 129.8, 129.6, 128.7, 127.3, 127.2, 53.0, 45.3. MS (ESI+): 359 [M − HBr_2]. Anal. ($C_{21}H_{20}Br_2N_4S$) C, H, Br, N, S.

General Procedure for Hydrochloride Iminothiadiazole Synthesis.[44] To the corresponding thiourea (1 equiv) in CH_2Cl_2 *N*-chlorosuccinimide (1.1 equiv) was added. The mixture was stirred for 2 h at room temperature. Then water (200 mL) and AcOEt (200 mL) were added. The organic layer was washed with water and dried over $MgSO_4$, and the solvent was removed under reduced pressure. The product was recrystallized from MeOH/H_2O.

5-(2-Hydroxyethylimino)-2,3-diphenyl-2,5-dihidro-1,2,4-thiadiazole Hydrochloride (52). Imidoylthiourea **3** (0.600 g, 2.00 mmol) and *N*-chlorosuccinimide (0.290 g, 2.20 mmol). Reaction time: 2 h. White solid (320 mg, 48%); mp 177−179 °C. ^{1}H NMR (DMSO) δ 10.57 (t, J = 5.6 Hz, 1H), 7.68−7.17 (m, 10H), 5.00 (bs, 1H), 3.77 (q, J = 5.5 Hz, 2H), 3.66 (t, J = 5.5, 2H). ^{13}C NMR (DMSO) δ 176.7, 165.3, 135.3, 133.1, 131.2, 130.8, 130.8, 129.3, 128.2, 127.6, 59.6, 48.1. ^{15}N NMR (DMSO) δ 131, 201, 247. MS (ESI+): 298 [M − Cl]. Anal. ($C_{16}H_{16}ClN_3OS$) C, H, Cl, N, S.

3-(1-Naphthyl)-2-phenyl-5-(3-pyridylmethylimino)-2,5-dihydro-1,2,4-thiadiazole Hydrochloride (53). Imidoylthiourea **21** (0.600 g, 1.51 mmol) and *N*-chlorosuccinimide (0.22 g, 1.66 mmol). Reaction time: 1 h. White solid (208 mg, 32%); mp 204−205 °C. ^{1}H NMR (DMSO) δ 11.03 (s, 1H), 8.66 (m, 1H), 8.55(m, 1H), 8.0−7.4 (m, 14H), 4.94 (s, 2H). ^{13}C NMR (DMSO) δ 176.8, 165.3, 144.6, 135.3, 133.1, 131.2, 130.8, 130.8, 129.3, 128.2, 127.6, 44.1. MS (ESI+): 395 [M − Cl]. Anal. ($C_{25}H_{20}ClN_4S$) C, H, Cl, N, S.

3-(4-Methoxyphenyl)-5-pentylimino-2-phenyl-2,5-dihydro-1,2,4-thiadiazole Hydrochloride (54). Imidoylthiourea **16** (0.600 g, 1.69 mmol) and *N*-chlorosuccinimide (0.25 g, 1.85 mmol). Reaction time: 2 h. Pale-yellow solid (185 mg, 28%); mp 138−139 °C. ^{1}H NMR (DMSO) δ 10.60 (t, J = 5.2, 1H), 7.62−7.5 (m, 5H), 7.4 (d, J = 8.3 Hz, 2H), 6.8 (d, J = 8.3 Hz, 2H), 3.78 (s, 3H), 3.71 (m, 2H), 1.71 (m, 2H), 1.42−1.32 (m, 4H), 0.91 (t, J = 7.2 Hz, 3H). ^{13}C NMR (DMSO) δ 175.4, 164.7, 162.8, 135.3, 133.1, 131.2, 130.8, 130.8, 129.3, 128.2, 127.6, 119.3, 114.5, 56.0, 44.9, 28.7, 28.4, 22.0, 14.2. MS (ESI+): 354 [M − Cl]. Anal. ($C_{20}H_{24}ClN_3OS$) C, H, Cl, N, S.

General Procedure for Iminothiadiazole Synthesis. To the corresponding thiourea (1 equiv) in CH_2Cl_2 *N*-chlorosuccinimide (1.1 equiv) was added. The mixture was stirred for 2 h at room temperature. Then water (200 mL) and AcOEt (200 mL) were added. The organic layer was washed with a $NaHCO_3$ saturated solution, dried over $MgSO_4$, and the solvent was removed under reduced pressure. The product was recrystallized from MeOH/H_2O.

2,3-Diphenyl-5-phenylimino-2,5-dihydro-1,2,4-thiadiazole (56). Imidoylthiourea **6** (0.41 g, 1.24 mmol) and *N*-chlorosuccinimide (0.18 g, 1.36 mmol). Reaction time: 2 h. Yellow solid (131 mg, 32%); mp 143−144 °C. (lit.[20] 141−142 °C). ^{1}H NMR (DMSO) δ 7.93−7.61 (m, 2H), 7.63−7.27 (m, 11H), 7.23−6.55 (m, 2H). ^{13}C NMR (DMSO) δ 167.5, 160.6, 159.6, 139.4, 136.7, 136.2, 134.4, 129.7, 129.1, 128.6, 128.5, 128.0, 127.2, 126.1, 125.7, 125.1, 124.6, 122.4, 121.5, 120.6, 120.4. MS (ESI+): 330 [M + H]. Anal. ($C_{20}H_{15}N_3S$) C, H, N, S.

5-Ethoxycarboximethylimino-2,3-diphenyl-2,5-dihydro-1,2,4-thiadiazole (57). Imidoylthiourea **2** (0.50 g, 1.46 mmol) and *N*-chlorosuccinimide (0.22 g, 1.61 mmol). Reaction time: 2 h. Orange solid (321 mg, 65%); mp 151−152 °C. ^{1}H NMR (DMSO) δ 8.11−7.93 (m, 2H), 7.72−6.89 (m, 8H), 5.36 (s, 2H, CH_2-N═), 4.42−4.17 (m, 1H, *E*-CH_2), 4.13 (q, J = 7.1 Hz, 1H, *Z*-CH_2), 1.47−1.17 (m, 1.5H *E*-CH_3), 1.20−0.81 (m, 1.5H, *Z*-CH_3). ^{13}C NMR (DMSO) δ 168.9, 167.3, 161.6, 161.2, 148.2, 136.1, 134.9, 132.4, 130.2, 129.1, 127.9, 126.7, 119.5, 62.0 (*E*-CH_2), 59.8 (*Z*-CH_2), 46.8 (CH_2), 14.4 (CH_3). MS (ESI+): 340 [M + H]. Anal. ($C_{18}H_{17}N_3O_2S$) C, H, N, S.

2-(*N*-Phenylbenzimidoyl)imino-2-hydro-(1,2,4)thiadiazolo-[2,3-*a*]pyridine (59). To the Imidoylthiourea **27** (0.55 g, 1.65 mmol) in CH_2Cl_2, *N*-chlorosuccinimide (0.24 g, 1.80 mmol) was added. The mixture was stirred for 3 h at room temperature. Then water (200 mL) and AcOEt (200 mL) were added. The organic layer was washed with water and dried over $MgSO_4$, and the solvent was removed under reduced pressure. The product was purified with several methanol washes to afford a yellow solid (108 mg, 20%); mp 238−239 °C. ^{1}H NMR (DMSO) δ 8.70−8.60 (m, 1H), 7.89 (ddd, J = 8.6, 7.0, 1.6 Hz, 1H), 7.61−7.47 (m, 3H), 7.48−7.29 (m, 6H), 7.29−7.17 (m, 2H), 7.15−6.98 (m, 1H). ^{13}C NMR (DMSO) δ 170.0, 161.5, 155.5, 138.4, 138.0, 137.4, 130.8, 130.7, 129.6, 129.4, 128.3, 127.5, 126.6, 119.2, 115.7. MS (ESI+): 331 [M + H]. Anal. ($C_{19}H_{14}N_4S$) C, H, N, S.

Molecular Modeling. Initial protein structures were set up with help of Sybyl 8.0[45] software adding hydrogens, removing ligands, cofactors, waters, and capping N and C-terminal residues and finally removing clashes and amide bumps. To carry out blind docking experiments, the resulting proteins structures were used with Autodock 4.2.2.1 software.[46] To this end, grids of points covering the whole protein were generated with ADT.[47] Box size: 126 × 126 × 126 points with a standard space of 0.375 Å. The center of the box is the protein center. Then Lamarckian genetic algorithm was chosen with default parameters except "Number of GA runs", "Population size" and "Maximum number of evals," which were set to 100, 100, and 3×10^6, respectively. The resulting docking solutions were clustered (within the default 2.0 Å rmsd), and only the most populated cluster in each protein structure was considered for further analysis. Visual inspection of solutions for all ligands in all structures led us to select only the solutions obtained for structure 1Q4L, which provided a common binding mode for all ligands compatible with the substrate binding site. Finally, the most interesting complexes were minimized with MMFF94 force field implemented in Sybyl 8.0 until a 0.01 kcal/mol gradient was reached in order to carry out a detailed analysis.

Biology. *Inhibition of GSK-3.* Human recombinant GSK-3β was purchased from Millipore (Millipore Iberica S.A.U.) The prephosphorylated polypeptide substrate was purchased from Millipore (Millipore Iberica SAU). Kinase-Glo Luminescent Kinase Assay was obtained from Promega (Promega Biotech Ibérica, SL). ATP and all other reagents were from Sigma-Aldrich (St. Louis, MO). Assay buffer contained 50 mM

HEPES (pH 7.5), 1 mM EDTA, 1 mM EGTA, and 15 mM magnesium acetate.

The method of Baki et al.[48] was followed to analyze the inhibition of GSK-3β. Kinase-Glo assays were performed in assay buffer using black 96-well plates. In a typical assay, 10 μL (10 μM) of test compound (dissolved in dimethyl sulfoxide [DMSO] at 1 mM concentration and diluted in advance in assay buffer to the desired concentration) and 10 μL (20 ng) of enzyme were added to each well followed by 20 μL of assay buffer containing 25 μM substrate and 1 μM ATP. The final DMSO concentration in the reaction mixture did not exceed 1%. After a 30 min incubation at 30 °C, the enzymatic reaction was stopped with 40 μL of Kinase-Glo reagent. Glow-type luminescence was recorded after 10 min using a FLUOstar Optima (BMG Labtechnologies GmbH, Offenburg, Germany) multimode reader. The activity is proportional to the difference of the total and consumed ATP. The inhibitory activities were calculated on the basis of maximal activities measured in the absence of inhibitor. The IC_{50} was defined as the concentration of each compound that reduces a 50% the enzymatic activity with respect to that without inhibitors.

Kinetic Studies on GSK-3β. To investigate the inhibitory mechanism of ITDZs on GSK-3β, several kinetic experiments were performed. Lineweaver−Burk plots of enzyme kinetics are shown in different figures in the previous text.

Kinetic experiments varying both GS-2 (from 15.5 to 100 μM) and ITDZs (from 0.5 to 2.5 μM) concentrations were performed. Double-reciprocal plotting of the data is depicted in Figure 4.

Kinetic experiments varying both ATP (from 1 to 50 μM) and ITDZs (from 0.4 to 2 μM) concentrations were performed using the ADP-Glo Kinase Assay.[49]

GSK-3 Reversibility Studies. To study the type of enzymatic inhibition for the compounds, assays were performed to determine the activity of the enzyme after several times of incubation of the enzyme with the inhibitor. A reversible inhibitor does not increase the inhibition of the enzyme with the time of incubation, while an irreversible inhibitor increases the inhibition percentage as the time of incubation with the enzyme increases.

Primary Cell Cultures. Cortical neurons were isolated from the cerebral cortex of E18 rats as previously described (Luna-Medina et al.)[50] Briefly, after dissecting the cerebral cortex, cells were seeded onto 96-well plates and cultures maintained in Neurobasal medium with B-27 supplements under humidified 5% CO_2 and 95% air at 37 °C. After 1 week in culture, cells were treated with the supernatant obtained from LPS-stimulated microglial cultures. Some of the cultures were pretreated for 1 h with the indicated compounds.

Astrocytes were prepared from neonatal (P2) rat cerebral cortex, as previously described by Luna-Medina et al.[50] Briefly, after removal of the meninges, the cerebral cortex was dissected, dissociated, and incubated with 0.25% trypsin/EDTA at 37 °C for 1 h. After centrifugation, the pellet was washed 3 times with HBSS (Gibco) and the cells were placed on noncoated flasks and maintained in HAMS/DMEM (1:1) medium containing 10% FBS. After 15 days, the flasks were agitated on an orbital shaker for 4 h at 240 rpm at 37 °C, the supernatant was collected, centrifuged, and the cellular pellet containing the microglial cells resuspended in complete medium (HAMS/DMEM (1:1) containing 10% FBS) and seeded on uncoated 96-well plates. Cells were allowed to adhere for 2 h, and the medium was removed to eliminate nonadherent oligodendrocytes. New fresh medium containing 10 ng/mL of GM-CSF was added. The remaining astroglial cells adhered on the flasks were then trypsinized, collected, centrifugated, and plated onto 96-well plates with complete medium. The purity of cultures obtained by this procedure was >98% as determined by immunofluorescence with the OX42 (microglial marker) and the GFAP (astroglial marker) antibodies.

Nitrites Measurement. Accumulation of nitrites in media was assayed by the standard Griess reaction. After stimulation of cells with the different compounds, supernatants were collected and mixed with an equal volume of Griess reagent (Sigma). Samples were then incubated at room temperature for 15 min and absorbance read using a plate reader at 492/540 nm.

Neurosphere Cultures. Neurosphere (NS) cultures were derived from the hippocampus of adult rats and induced to proliferate using established passaging methods to achieve optimal cellular expansion according to published protocols.[51] Rats were decapitated, brains removed, and the hippocampus dissected as described.[52] Briefly, cells were seeded into 12-well dishes and cultured in Dubecco's Modified Eagle's Medium (DMEM)/F12 (1:1, Invitrogen) containing 10 ng/mL epidermal growth factor (EGF, Peprotech, London, UK), 10 ng/mL fibroblast growth factor (FGF, Peprotech), and B27 medium (Gibco). After 3 days in culture, some primary NS cultures were treated with different GSK-3β inhibitors. To determine the ability of GSK-3 to induce differentiation, NS from 10-day old cultures were plated for 72 h onto 100 μg/mL poly-L-lysine-coated coverslips in the absence of exogenous growth factors. Then, cells were processed for immunocytochemistry for β-tubulin to identify neurons.

Immunocytochemistry. Cells were processed for immunocytochemistry as previously described.[50] Briefly, at the end of the treatment period, NS cultures were grown on glass coverslips in 24-well cell culture plates. Cultures were then washed with phosphate-buffered saline (PBS) and fixed for 30 min with 4% paraformaldehyde at 25 °C and permeabilized with 0.1% Triton X-100 for 30 min at 37 °C. After 1 h incubation with the corresponding primary antibody, cells were washed with phosphate-buffered saline and incubated with an Alexa-labeled secondary antibody (Molecular Probes; Leiden, The Netherlands) for 45 min at 37 °C. Later on, images were obtained using a TCS SP5 laser scanning spectral confocal microscope (Leica Microsystems). Confocal microscope settings were adjusted to produce the optimum signal-to-noise ratio. The primary antibody used was a polyclonal anti-β-tubulin (clone Tuj1; Abcam). Dapi staining was used as a nuclear marker.

In Vitro Parallel Artificial Membrane Permeability Assay (PAMPA). Prediction of the brain penetration was evaluated using a parallel artificial membrane permeability assay (PAMPA). Ten commercial drugs, phosphate buffer saline solution at pH 7.4 (PBS), DMSO, and dodecane were purchased from Sigma, Acros organics, Aldrich, and Fluka. The porcine polar brain lipid (PBL) (catalogue no. 141101) was from Avanti Polar Lipids. The donor plate was a 96-well filtrate plate (Multiscreen IP Sterile Plate PDVF membrane, pore size is 0.45 μM, catalogue no. MAIPS4510), and the acceptor plate was an indented 96-well plate (Multiscreen, catalogue no. MAMCS9610), both from Millipore. Filter PDVF membrane units (diameter 30 mm, pore size 0.45 μm) from Symta were used to filtered the samples. A 96-well plate UV reader (Thermoscientific, Multiskan spectrum) was used for the UV measurements. Test compounds [(3−5 mg of caffeine, enoxacine, hydrocortisone, desipramine, ofloxacine, piroxicam, and testosterone), (12 mg of promazine), and 25 mg of verapamil and atenolol] were dissolved in DMSO (250 μL). Then 25 μL of this compound stock solution was taken, and 225 μL of DMSO and 4750 μL of PBS pH 7.4 buffer were added to reach 5% of DMSO concentration in the experiment. These solutions were filtered. The acceptor 96-well microplate was filled with 180 μL of PBS:DMSO (95:5). The donor 96-well plate was coated with 4 μL of porcine brain lipid in dodecane (20 mg mL^{-1}), and after 5 min, 180 μL of each compound solution was added. Then 1−2 mg of every compound to be determined for their ability to pass the brain barrier were dissolved in 250 μL of DMSO and 4750 μL of PBS pH 7.4 buffer, filtered, and then added to the donor 96-well plate. Then the donor plate was carefully put on the acceptor plate to form a "sandwich", which was left undisturbed for 4 h at 25 °C. During this time, the compounds diffused from the donor plate through the brain lipid membrane into the acceptor plate. After incubation, the donor plate was removed. The concentration of compounds and commercial drugs in the acceptor and the donor wells was determined by UV plate reader. Every sample was analyzed at three to five wavelengths, in three wells and in three independent runs. Results are given as the mean [standard deviation (SD)], and the average of the three runs is reported. Ten quality control compounds (previously mentioned) of known BBB permeability were included in each experiment to validate the analysis set.

■ ASSOCIATED CONTENT

Supporting Information

Elemental analyses of compounds **28**−**59**, NMR data ($^{15}N-^{1}H$ HMBC, $^{13}C-^{1}H$ HMBC, and NOE experiment) for compounds **29**, **28**, and **55**, linear correlation between experimental and reported permeability of commercial drugs using the PAMPA-BBB assay. This material is available free of charge via the Internet at http://pubs.acs.org.

■ AUTHOR INFORMATION

Corresponding Author

*Phone: +34915680010. Fax: +34915644853. E-mail: amartinez@iqm.csic.es or cgil@iqm.csic.es.

Notes

The authors declare no competing financial interest.

■ ACKNOWLEDGMENTS

We gratefully acknowledge the financial support of Ministry of Science and Innovation (MICINN, projects no. SAF2009-13015-C02-01, to A.M. and SAF2010-16365, to A.P-C.), and FECYT, project no. INC-0367, to A.M.) and Instituto de Salud Carlos III (ISCiii, project no. RD07/0060/0015). V.P. and D.I.P. acknowledge pre- and postdoctoral fellowships respectively from CSIC (JAE program). This work has been awarded with "Ramon Madroñero" prize for novel researchers from SEQT.

■ ABBREVIATIONS USED

ITDZ, iminothiadiazoles; GSK-3, glycogen synthase kinase 3; AD, Alzheimer's disease; TDZD, thiadiazolidindiones; PDB, Protein Data Bank; CNS, central nervous system

■ REFERENCES

(1) Cohen, P.; Yellowlees, D.; Aitken, A.; Donella-Deana, A.; Hemmings, B. A.; Parker, P. J. Separation and characterisation of glycogen synthase kinase 3, glycogen synthase kinase 4 and glycogen synthase kinase 5 from rabbit skeletal muscle. *Eur. J. Biochem.* **1982**, *124*, 21−35.

(2) Martinez, A.; Castro, A.; Medina, M.; Eds. In *Glycogen Synthase Kinase 3 and Its Inhibitors*; John Wiley & Sons: New York, 2006.

(3) Rayasam, G. V.; Tulasi, V. K.; Sodhi, R.; Davis, J. A.; Ray, A. Glycogen synthase kinase 3: more than a namesake. *Br. J. Pharmacol.* **2009**, *156*, 885−898.

(4) Kannoji, A.; Phukan, S.; Sudher Babu, V.; Balaji, V. N. GSK3beta: a master switch and a promising target. *Expert Opin. Ther. Targets* **2008**, *12*, 1443−1455.

(5) Hooper, C.; Killick, R.; Lovestone, S. The GSK3 hypothesis of Alzheimer's disease. *J. Neurochem.* **2008**, *104*, 1433−1439.

(6) Li, X.; Jope, R. S. Is glycogen synthase kinase-3 a central modulator in mood regulation? *Neuropsychopharmacology* **2010**, *35*, 2143−2154.

(7) Martinez, A.; Perez, D. I. GSK-3 inhibitors: a ray of hope for the treatment of Alzheimer's disease? *J. Alzheimer's Dis.* **2008**, *15*, 181−191.

(8) Martinez, A.; Gil, C.; Perez, D. I. Glycogen synthase kinase 3 inhibitors in the next horizon for Alzheimer's disease treatment. *Int. J. Alzheimer's Dis.* **2011**, DOI: 10.4061/2011/280502.

(9) Jope, R. S. Glycogen synthase kinase-3 in the etiology and treatment of mood disorders. *Front. Mol. Neurosci.* **2011**, *4*, 16 DOI: 10.3389/fnmol.2011.00016.

(10) Eglen, R.; Reisine, T. Drug discovery and the human kinome: recent trends. *Pharmacol. Ther.* **2011**, *130*, 144−156.

(11) Eglen, R. M.; Reisine, T. The current status of drug discovery against the human kinome. *Assay Drug Dev. Technol.* **2009**, *7*, 22−43.

(12) Chico, L. K.; Van Eldik, L. J.; Watterson, D. M. Targeting protein kinases in central nervous system disorders. *Nature Rev. Drug Discovery* **2009**, *8*, 892−909.

(13) Eldar-Finkelman, H.; Martinez, A. GSK-3 inhibitors: preclinical and clinical focus on CNS. *Front. Mol. Neurosci.* **2011**, *4*, 32 DOI: 10.3389/fnmol.2011.00032.

(14) Martinez, A.; Alonso, M.; Castro, A.; Perez, C.; Moreno, F. J. First non-ATP competitive glycogen synthase kinase 3 beta (GSK-3beta) inhibitors: thiadiazolidinones (TDZD) as potential drugs for the treatment of Alzheimer's disease. *J. Med. Chem.* **2002**, *45*, 1292−1299.

(15) del Ser, T. Phase IIa clinical trial on Alzheimer's disease with NP12, a GSK-3 inhibitor. *Alzheimer's Dementia* **2010**, *6*, S147.

(16) Eldar-Finkelman, H.; Licht-Murava, A.; Pietrokovski, S.; Eisenstein, M. Substrate competitive GSK-3 inhibitors—strategy and implications. *Biochim. Biophys. Acta* **2010**, *1804*, 598−603.

(17) Eldar-Finkelman, H.; Eisenstein, M. Peptide inhibitors targeting protein kinases. *Curr. Pharm. Des.* **2009**, *15*, 2463−2470.

(18) Martinez, A.; Alonso, M.; Castro, A.; Dorronsoro, I.; Gelpi, J. L.; Luque, F. J.; Perez, C.; Moreno, F. J. SAR and 3D-QSAR studies on thiadiazolidinone derivatives: exploration of structural requirements for glycogen synthase kinase 3 inhibitors. *J. Med. Chem.* **2005**, *48*, 7103−7112.

(19) Castro, A.; Encinas, A.; Gil, C.; Brase, S.; Porcal, W.; Perez, C.; Moreno, F. J.; Martinez, A. Non-ATP competitive glycogen synthase kinase 3beta (GSK-3beta) inhibitors: study of structural requirements for thiadiazolidinone derivatives. *Bioorg. Med. Chem.* **2008**, *16*, 495−510.

(20) Goerdeler, J.; Lobach, W. Reaktionen von 5-imino-Δ3-1,2,4-thiadiazolinen mit heterocumulenen (Präparative Gesichtspunkte). *Chem. Ber.* **1979**, *112*, 517−531.

(21) Göblyös, A.; de Vries, H.; Brussee, J.; Ijzerman, A. P. Synthesis and biological evaluation of a new series of 2,3,5-substituted [1,2,4]-thiadiazoles as modulators of adenosine A1 receptors and their molecular mechanism of action. *J. Med. Chem.* **2005**, *48*, 1145−1151.

(22) Polgar, T.; Baki, A.; Szendrei, G. I.; Keseru, G. M. Comparative virtual and experimental high-throughput screening for glycogen synthase kinase-3beta inhibitors. *J. Med. Chem.* **2005**, *48*, 7946−7959.

(23) Dutta, S.; Burkhardt, K.; Young, J.; Swaminathan, G. J.; Matsuura, T.; Henrick, K.; Nakamura, H.; Berman, H. M. Data deposition and annotation at the worldwide protein data bank. *Mol. Biotechnol.* **2009**, *42*, 1−13.

(24) Palomo, V.; Soteras, I.; Perez, D. I.; Perez, C.; Campillo, N. E.; Gil, C.; Martinez, A. Exploring the binding sites of glycogen synthase kinase 3. Identification and characterization of allosteric modulation cavities. *J. Med. Chem.* **2011**, *54*, 8461−8470.

(25) Perez, D. I.; Palomo, V.; Perez, C.; Gil, C.; Dans, P. D.; Luque, F. J.; Conde, S.; Martinez, A. Switching reversibility to irreversibility in glycogen synthase kinase 3 inhibitors: clues for specific design of new compounds. *J. Med. Chem.* **2011**, *54*, 4042−4056.

(26) Peng, J.; Kudrimoti, S.; Prasanna, S.; Odde, S.; Doerksen, R. J.; Pennaka, H. K.; Choo, Y. M.; Rao, K. V.; Tekwani, B. L.; Madgula, V.; Khan, S. I.; Wang, B.; Mayer, A. M.; Jacob, M. R.; Tu, L. C.; Gertsch, J.; Hamann, M. T. Structure−activity relationship and mechanism of action studies of manzamine analogues for the control of neuro-inflammation and cerebral infections. *J. Med. Chem.* **2010**, *53*, 61−76.

(27) Imai, Y. N.; Inoue, Y.; Nakanishi, I.; Kitaura, K. Amide−pi interactions between formamide and benzene. *J. Comput. Chem.* **2009**, *30*, 2267−2276.

(28) Ringer, A. L.; Senenko, A.; Sherrill, C. D. Models of S/pi interactions in protein structures: comparison of the H2S benzene complex with PDB data. *Protein Sci.* **2007**, *16*, 2216−2223.

(29) Cubero, E.; Luque, F. J.; Orozco, M. Is polarization important in cation−-pi interactions? *Proc. Natl. Acad. Sci. U.S.A.* **1998**, *95*, 5976−5980.

(30) Blanco, F.; Kelly, B.; Alkorta, I.; Rozas, I.; Elguero, J. Cation−pi interactions: complexes of guanidinium and simple aromatic systems. *Chem. Phys. Lett.* **2011**, *511*, 129−134.

(31) Morrison, R. S.; Kinoshita, Y.; Johnson, M. D.; Ghatan, S.; Ho, J. T. Garden, G. Neuronal survival and cell death signaling pathways. *Adv. Exp. Med. Biol.* **2002**, *513*, 41−86.
(32) Beurel, E.; Jope, R. S. Glycogen synthase kinase-3 regulates inflammatory tolerance in astrocytes. *Neuroscience* **2011**, *169*, 1063−1070.
(33) Morales-Garcia, J. A.; Luna-Medina, R.; Alonso-Gil, S.; Sanz-SanCristobal, M.; Palomo, V.; Gil, C.; Martinez, A.; Santos, A.; Perez-Castillo, A. Glycogen synthase kinase 3β inhibition promotes adult hippocampal neurogenesis in vitro and in vivo. *Neurobiol. Dis.* **2011**, submitted for publication.
(34) Nielsen, P. A.; Andersson, O.; Hansen, S. H.; Simonsen, K. B.; Andersson, G. Models for predicting blood−brain barrier permeation. *Drug Discovery Today* **2011**, *16*, 472−475.
(35) Di, L.; Kerns, E. H.; Fan, K.; McConnell, O. J.; Carter, G. T. High throughput artificial membrane permeability assay for blood−brain barrier. *Eur. J. Med. Chem.* **2003**, *38*, 223−232.
(36) Crivori, P.; Cruciani, G.; Carrupt, P. A.; Testa, B. Predicting blood−brain barrier permeation from three-dimensional molecular structure. *J. Med. Chem.* **2000**, *43*, 2204−2216.
(37) Paterniti, I.; Mazzon, E.; Gil, C.; Impllizzari, D.; Palomo, V.; Redondo, M.; Perez, D. I.; Esposito, E.; Martinez, A.; Cuzzocrea, S. PDE 7 inhibitors: new potential drugs for the therapy of spinal cord injury. *PLoS ONE* **2011**, *6*, e15937.
(38) Perez, D. I.; Pistolozzi, M.; Palomo, V.; Redondo, M.; Fortugno, C.; Gil, C.; Felix, G.; Martinez, A.; Bertucci, C. 5-Imino-1,2-4-thiadiazoles and Quinazolines derivatives as Glycogen Synthase Kinase 3β (GSK-3β) and Phosphodiesterase 7 (PDE7) Inhibitors: Determination of Blood−Brain Barrier Penetration and Binding to Human Serum Albumin. *Eur. J. Pharm. Sci.* **2012**, DOI: 10.1016/j.ejps.2012.01.007.
(39) Claramunt, R. M.; Maria, D. S.; Pinilla, E.; Torres, M. R.; Elguero, J. Structural studies of two Tinuvin P analogs: 2-(2,4-dimethylphenyl)-2*H*-benzotriazole and 2-phenyl-2*H*-benzotriazole. *Molecules* **2007**, *12*, 2201−2214.
(40) Cunico, R. F.; Pandey, R. K. Palladium-catalyzed synthesis of alpha-iminoamides from imidoyl chlorides and a carbamoylsilane. *J. Org. Chem.* **2005**, *70*, 5344−5346.
(41) Zyabrev, V. S.; Kharchenko, A. V.; Pirozhenko, V. V.; Drach, B. S. Acylation of 5-amino-2-aryl-3-phenyl-1,24-thiadiazolium chlorides. *Zh. Org. Khim.* **1988**, *24*, 1754−1762.
(42) Barnikow, G.; Ebeling, H. Isothiocyanates. 32. Reaction of imidoyl isothiocyanates with 2-aminothiazole. *Z. Chem.* **1973**, *13*, 468−468.
(43) Zyabrev, V. S.; Rensky, M. A.; Rusanov, E. B.; Drach, B. S. Cycloaddition of *N*-(2,2,2-trichloroethylidene)-substituted carboxamides and carbamates to 1,2,4-thiadiazol-5(2*H*)-imines. *Heteroat. Chem* **2003**, *14*, 474−480.
(44) Chetia, J. P.; Mazumder, S. N.; Mahajan, M. P. One-pot synthesis of 2-aryl-3-phenyl(benzyl)-5-phenylimino-1,2,4-thiadiazolines using *N*-chlorosuccinimide. *Synthesis* **1985**, 83−84.
(45) *SYBYL 8.0*; Tripos International: 1699 South Hanley Rd., St., Louis, MO 63144 USA.
(46) Morris, G. M.; Goodsell, D. S.; Halliday, R. S.; Huey, R.; Hart, W. E.; Belew, R. K.; Olson, A. J. Automated docking using a Lamarckian genetic algorithm and an empirical binding free energy function. *J. Comput. Chem.* **1998**, *19*, 1639−1662.
(47) Sanner, M. F. Python: a programming language for software integration and development. *J. Mol. Graph. Model.* **1999**, *17*, 57−61.
(48) Baki, A.; Bielik, A.; Molnar, L.; Szendrei, G.; Keseru, G. M. A high throughput luminescent assay for glycogen synthase kinase-3beta inhibitors. *Assay Drug Dev. Technol.* **2007**, *5*, 75−83.
(49) *ADP-Glo Kinase Assay Technical Manual*; www.promega.com/tbs/.
(50) Luna-Medina, R.; Cortes-Canteli, M.; Alonso, M.; Santos, A.; Martinez, A.; Perez-Castillo, A. Regulation of inflammatory response in neural cells in vitro by thiadiazolidinones derivatives through peroxisome proliferator-activated receptor gamma activation. *J. Biol. Chem.* **2005**, *280*, 21453−21462.
(51) Ferron, S. R.; Andreu-Agullo, C.; Mira, H.; Sanchez, P.; Marques-Torrejon, M. A.; Farinas, I. A combined ex/in vivo assay to detect effects of exogenously added factors in neural stem cells. *Nature Protoc.* **2007**, *2*, 849−859.
(52) Morales-Garcia, J. A.; Luna-Medina, R.; Alfaro-Cervello, C.; Cortes-Canteli, M.; Santos, A.; Garcia-Verdugo, J. M.; Perez-Castillo, A. Peroxisome proliferator-activated receptor gamma ligands regulate neural stem cell proliferation and differentiation in vitro and in vivo. *Glia* **2011**, *59*, 293−307.